Universidade de Aveiro Departamento de Biologia
2019

Inês de Almeida Mendes Marques de Carvalho

Mercury effect on embryonic development of Zebrafish

Efeito do mercúrio no desenvolvimento embrionário do peixe zebra

DECLARAÇÃO

Declaro que este relatório é integralmente da minha autoria, estando devidamente referenciadas as fontes e obras consultadas, bem como identificadas de modo claro as citações dessas obras. Não contém, por isso, qualquer tipo de plágio quer de textos publicados, qualquer que seja o meio dessa publicação, incluindo meios eletrónicos, quer de trabalhos académicos.

Universidade de Aveiro Departamento de Biologia
2019

Inês de Almeida Mendes Marques de Carvalho

Mercury effect on embryonic development of Zebrafish

Efeito do mercúrio no desenvolvimento embrionário do peixe zebra

Dissertação apresentada à Universidade de Aveiro para cumprimento dos requisitos necessários à obtenção do grau de Mestre em Biologia Aplicada, realizada sob a orientação científica da Doutora Susana Loureiro, Professora Auxiliar com Agregação do Departamento de Biologia da Universidade de Aveiro e da Doutora Margarida Fardilha, Professora Auxiliar com Agregação do Departamento de Ciências Médicas da Universidade de Aveiro

o júri

presidente

Prof.ª Doutora Maria Adelaide de Pinho Almeida
Professora auxiliar com agregação da Universidade de Aveiro

Doutora Marta Sofia Soares Craveiro Alves Monteiro dos Santos
Investigadora do CESAM- Centro de Estudos do Ambiente e do Mar da Universidade de Aveiro.

Prof.ª Doutora Susana Patrícia Mendes Loureiro
Professora auxiliar com agregação da Universidade de Aveiro

agradecimentos

Estes últimos anos foram de desafio, construção, amadurecimento e conquista pessoal. Nada era possível sem aqueles que, de forma direta ou indireta, individual ou coletiva, colaboraram no sentido de possibilitar este trabalho de investigação. Guardo um profundo sentimento de agradecimento para com todas as pessoas que fizeram parte deste percurso.

Às professoras Susana Loureiro e Margarida Fardilha pela orientação, apoio, confiança e competência que sempre demonstraram, e pela oportunidade de poder desenvolver este projeto.
À Maria Pavlaki, Magda Henriques e Cátia Santos por toda a ajuda, disponibilidade e paciência nestes meses de trabalho.

À minha mãe heroína pelo amor e apoio que me deu, pelas palavras de incentivo, otimismo e orgulho que me transmitiu nos nossos momentos.
Ao meu pai que me fortaleceu, pela sua forma exigente, crítica e criativa, e que para mim foi muito importante.
Ao meu irmão pela amizade e paciência com que me apoiou não só no período de elaboração desta tese, mas ao longo da vida.
Ao meu avô pela sua amabilidade e gentileza, que mesmo estando longe esteve sempre presente.
À minha avó pela adorável companhia e pelo carinho que me permitiram terminar esta gratificante etapa.

Por fim, aos meus amigos, especialmente à Márcia Santos, Ana Patrícia, Elsa Ribeiro, Sara Pêgo, Rita Ferraz, Marta Rente, Nuno Verónico, Inês Andrade e Inês Cardoso que me apoiaram incondicionalmente e ajudaram a que este percurso fosse realizado com mais alegria.

Muito obrigado.

palavras-chave

Peixe-zebra, mercúrio, toxicologia, morfologia, stress oxidativo, neurotoxicidade, fertilidade.

resumo

O mercúrio (Hg) é um contaminante perigoso para selvagem ambiente e para a saúde humana. *Danio rerio* (peixe-zebra) é uma espécie modelo comum, usada em toxicologia e ecotoxicologia para estudar os efeitos de contaminantes na saúde humana e no ambiente. O objetivo deste estudo foi identificar os efeitos causados pela exposição ao mercúrio (Hg) no desenvolvimento embrionário do peixe-zebra e nos biomarcadores de efeito.

Os embriões de peixe-zebra foram expostos a diferentes concentrações de $HgCl_2$ (0, 10 e 100 µg/L) durante 96 horas após a fertilização (hpf). A toxicidade e os parâmetros de desenvolvimento foram avaliados a cada 24 horas durante o período de exposição. As alterações induzidas pelo Hg ao nível da colinesterase (ChE), catalase (CAT), glutationa-S-transferase (GST), glutationa-redutase (GR), fosfoproteína fosfatase-1-gama (PPP1CC) e glutationa peroxidase-4 (GPx4), foram avaliadas em ovos ou larvas de peixe-zebra, recolhidos e congelados antes da análise a cada 24 horas até às 96h.

Os resultados mostraram que 100 µg/L de Hg induzem alterações no desenvolvimento do peixe-zebra, incluindo várias malformações (por exemplo, edema do pericárdio e curvatura) e atraso no período de eclosão. Além disso, foi detetada uma diminuição significativa nos níveis de ChE (marcador neurotóxico), em indivíduos expostos a 100 µg/L de Hg, e foi observado um aumento nos níveis de atividade de GST (marcador de stress oxidativo). Pela primeira vez, foi avaliado o efeito do Hg nos níveis da PPP1CC e da GPx4 durante o desenvolvimento do peixe-zebra. Mostrou-se que os níveis de PPP1CC aumentam ao longo do desenvolvimento embrionário, no entanto, não foi detetada nenhuma alteração nos níveis da proteína após a exposição ao Hg. O nosso estudo mostrou que a exposição ao Hg induz alterações ao nível do desenvolvimento do peixe-zebra e dos biomarcadores de efeito.

keywords

Zebrafish, Mercury, toxicology, morphology, oxidative stress, neurotoxicity, fertility.

abstract

Mercury (Hg) is a widespread contaminant hazardous to the environment and human health. *Danio rerio* (zebrafish) is a common model species used in toxicology and ecotoxicology, as a surrogate model to understand the effects of contaminants on human health and the environment. The aim of this study was to identify the effects of mercury (Hg) exposure on zebrafish embryo development and biomarkers levels.

Zebrafish embryos were exposed to different concentrations of $HgCl_2$ (0, 10 and 100 µg/L) up to 96 hours post-fertilization (hpf). Toxicity and developmental endpoints were assessed every 24h during the exposure period. Hg-induced alterations in the levels of Cholinesterase (ChE), Catalase (CAT), Glutathione-S-transferase (GST), Glutathione-Reductase (GR), Phosphoprotein Phosphatase-1-gamma (PPP1CC) and Glutathione Peroxidase-4 (GPx4), were assessed in zebrafish eggs or larvae, collected and snap-frozen prior to analysis every 24h up to 96h.

Results showed that at 100 µg/L $HgCl_2$ induced developmental changes in zebrafish development, including several malformations (eg. Pericardial edema and curvature) and delay of the hatching period. Additionally, a significant decrease in ChE levels (marker of neurotoxic damage) was detected in individuals exposed to 100 µg/L of $HgCl_2$, while an increase in GST activity levels (marker of oxidative stress) was observed. For the first time, the effect of Hg on the levels of PPP1CC and GPx4 during zebrafish development was tested. Overall, we found levels of PPP1CC to increase over time. No alteration on protein levels following Hg exposure were, however, reported.

Taken together, our study showed that Hg exposure induced alterations at developmental and biomarkers levels.

Index

List of Figures

List of Tables

Abbreviations

Abreviatura	Descrição
AChE	Acetilcolinesterase
BChE	Butyrylcholinesterase
Ca^{2+}	Calcium ion
CAT	Catalase
ChE	Cholinesterase
dpf	day post fertilization
EU	European Union
GPx	Glutathione Peroxidase
GR	Glutathione Reductase
GSH	Glutathione
GSSG	Glutathione disulfide
GST	Glutathione S-Transferase
H_2O	Water
H_2O_2	Peroxide hydrogen
Hg	Mercury
Hg^0	Elemental mercury
HG^{II}	Ionic mercury
$HgCl_2$	Mercury chloride
HgS	Mercury sulfate
hpf	hour post-fertilization
HPG	Hypothalamic–Pituitary–Gonadal
LOOH	lipid hydroperoxide
MDA	malondialdehyde
MeHg	methylmercury
mRNA	Messenger Ribonucleic acid
NRC	National research council
O_2	Oxigen
PK	Protein Kinase
PPs	Protein Phosphatase
PPP1	Phosphoprotein phosphatase 1
PPP1CA	Phosphoprotein phosphatase 1 alpha
PPP1CB	Phosphoprotein phosphatase beta
PPP1CC	Phosphoprotein phosphatase gama
ROS	Reactive oxidative species
Ser/Thr	Serine and Threonine
SOD	Superoxide dismutase
STPPs	serine-threonine protein phosphatase
Tyr	Tyrosine

1.Introduction

1.1 Mercury biogeochemical cycle

Mercury (Hg) is a ubiquitous environmental pollutant (1). It can be present in elemental, inorganic (e.g. mercury sulfide (HgS), mercury chloride ($HgCl_2$)) and/or organic forms (e.g. methylmercury (MeHg)) in air, soil and water (2). Hg is naturally mobilized in Earth's biogeochemical system via volcanic activity and forest fires (3). Hg exists in small amounts in inorganic compounds in the mantle (mostly HgS) and the core of the earth. It is a volatile part of the volcanic activity that releases about 90 ton/yr of Hg for atmosphere (4).

Apart from that, the increase in temperature provoked by climate changes decreases the energy of the organisms, promoting a higher consumption rate and so an increase of MeHg in the organism (5). Furthermore, increases of wildfires rise the release of Hg present in terrestrial soils (6).

In spite of this, about half of the Hg mobilized to the atmosphere is resultant from anthropogenic activities such as coal-burning for energy production, incineration and is heavily used in the production of sodium hydroxide (Castner-Kellner process) and small-scale gold mining (7,8).

The first cases of human poisoning by MeHg (called Minamata disease) occurred in 1956, in Minamata and Niigata, Japan, and it was caused by the consumption of fish, affecting mainly the cerebrum and the cerebellum (9). This case had a global impact in the public awareness on Hg contamination and, efforts were made to identify and reduce contaminations by Hg included some industrial productions (eg. lamps) and medical applications (thermometers and disinfectants such as mercurochrome) (10,11).

Most industrial and medical applications have been banned in the European Union (EU) and many other countries (12), which enabled Hg emissions to decrease until 2014 by 73% and 71%, in air and water, respectively. Nowadays, the EU accounts for less than 5% global Hg air emissions, and overall Hg emission rate in the EU is expected to decrease by approximately more 40% until 2021 (13).

The Hg biogeochemical cycle is composed of interaction of atmospheric, terrestrial, aquatic and biotic compartments (14) (Figure 1).

Mercury is the only metal that is considered as a “global” pollutant because in its elemental form (Hg^0) has an atmospheric residence time of 0.8 months to 1.7 years, allowing it to travel for long distances (15). After releasing in the atmosphere, Hg^0 easily suffers

photochemical oxidation, forming water-soluble divalent Hg species (Hg^{II}) that are deposited into aquatic and terrestrial ecosystems (6), dissolving in water and constituting part of the rain and snow (16). Then, a part is reduced back to Hg^0 and reintroduced into the atmosphere, whereas the remainder Hg^{II} cycles through oceans and soils until it is re-sequestered into the lithosphere (6). In the ground, it rapidly makes several inorganic compounds such as HgS and $HgCl_2$ and accumulates until it is methylated by anaerobic bacteria such as sulfate-reducing bacteria converting Hg^{II} into MeHg (17). This process of methylation occurs also in muds, rivers, lakes, and oceans. MeHg easily enters in aquatic food web through algae, shellfish, bivalves, krill, etc. and readily bioaccumulates and biomagnifies (6,18). Thus, several Hg compounds are present in the human body (≈0.19 ppm), although they have no known vital or beneficial effect and over time can cause serious illnesses (19).

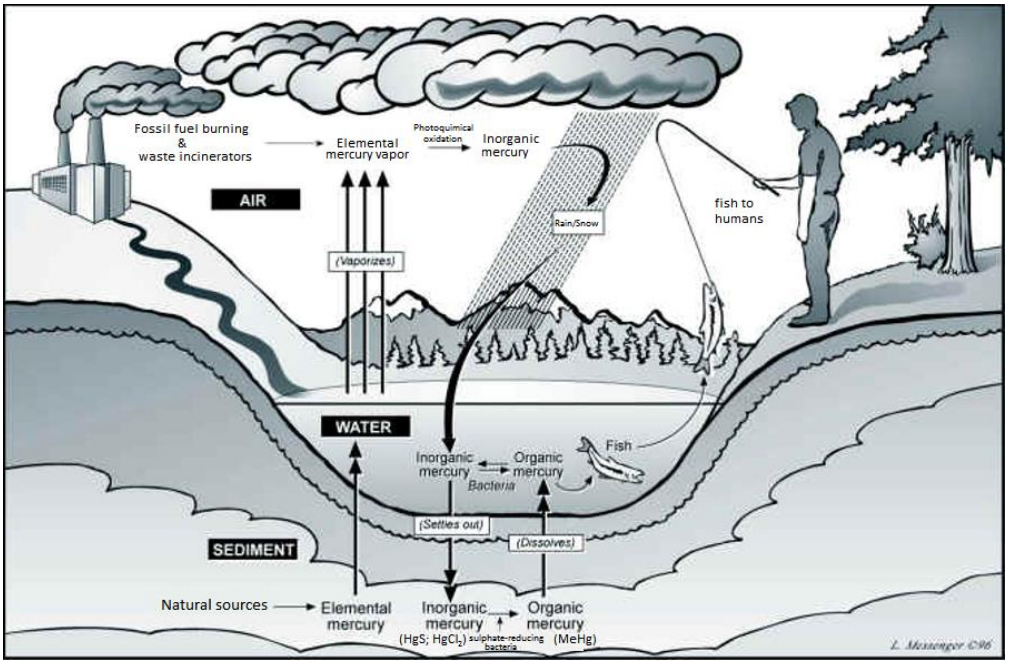

Figure 1: Mercury cycle in the environment (adapted from (17)*).*

1.2 Mercury toxicity to biota

Hg is highly toxic at low levels to both aquatic and terrestrial organisms (20). Hg is neurotoxic, affecting primarily the nervous system, which may lead to changes in behaviour, motor and sensory function in exposed organisms (21–23). Moreover, Hg can also induce

oxidative stress and damage in the immune system and alterations in reproduction, and survival in exposed animals and humans (20,24).

In the environment, one example of the effects of Hg exposure is in ria the Aveiro, that receives water from a highly contaminated effluent by a mercury cell chlor-alkali plant from the 1950s until 1994 (25). These contamination affected the quality of the soils in the area and the macrophyte harvesting for human direct or indirect use and the consumption of mussels, crabs and the sea bass from the Laranjo bay constituted a health risk (25,26).

In birds, the Hg exposure, has been linked to impaired immune and neurological function, reduced reproductive and hatching success, increase incidence of abnormal development and altered parental and chick behaviour (27,28). For example, in a study with white ibises (*Eudocimus albus*) exposed to environmentally relevant dietary MeHg concentrations, they made fewer nesting attempts, had lowered egg productivity and exhibited more same-sex pairing behaviour among males (27).

In humans, Hg exposure is immunotoxic, carcinogenic, and teratogenic (29). Continuous exposure to low Hg concentrations can lead to infertility and men with higher blood Hg concentrations showed poor sperm parameters than men with lower concentrations of Hg (30). Also in humans, exposure to Hg induced sperm DNA damage and menstrual disorders, spontaneous abortions, malformations and, stillbirth were associated with higher levels of maternal Hg exposure (31). In monkeys, studies showed that Hg decreased sperm motility and swimming speed and increased the abnormal sperm tail morphology (32).

A study with Wistar rats showed that at a Hg intake of 3.0 mg/kg body weight/day, Hg bioaccumulated in testis, epididymis, seminal vesicle, vas deferens, liver, and kidney, being the kidney the organ that showed the highest Hg concentrations. Moreover, this study showed that MeHg produced a significant reduction in serum testosterone levels at individuals with Hg intake of 3.0 mg/kg body weight/day (33). In rats, free radicals are involved in the control of steroidogenesis in Leydig cells so oxidative stress may be a cause of testicular steroidogenic disorder as free radicals prevent gonadal steroidogenesis (34,35). Studies showed that the increase of reactive oxygen species (ROS) and the inhibition of antioxidant enzymes activity can be related with the increase of abnormal reduction in the production of spermatozoa (36). In rats with 7 weeks old, it was showed that Hg decreases the testosterone levels and impaired spermatogenesis (37).

In mice with 12 weeks old, Hg exposure decreases the number of spermatozoa and the testicular weight (38). In female mice, Hg exposure resulted in an accumulation in ovaries that may be a cause of the alterations in reproductive function, contributing to infertility or ovarian failure (38). Moreover, evidences suggest that there is a transplacental passage of Hg in mice (39). This was also confirmed for humans, in the study of Alves et al (40), where levels of Hg were detected in both maternal and fetal parts of the placenta, as well in the amniotic membrane and umbilical cord.

In marine fish, the embryonic and larval stages are the most sensitive periods for Hg exposure (41). Studies showed that Hg-induced hepatotoxicity induced genetic mutations, oxidative stress, cytoskeletal damage, immunotoxicity and changes in energy metabolism, indicating that mitochondria may be the primary target for Hg in cells (41). MeHg also induce malformations mostly in the spine, behaviour changes and reducing the hatching success and survival. Moreover, Hg induced a decrease in the fish growth, once it is expended more energy to eliminate MeHg, accumulated in the brain, inducing changes in the total number and volume of neurons and glial cells in specific areas of the brain, leading to changes in swimming (42).

MeHg can accumulate in the gonads of fish and may affect the reproductive system and inhibit the growth and development of fish gonads (43). Hg interfered with the expression of genes related to the hypothalamic–pituitary–gonadal (HPG) axis, altering the sex hormone levels, making the gonadal tube walls thicker, detecting spermatogenic degeneration and necrosis (Sertoli cells suffered hypertrophy and occurred interstitial inflammation) and disrupting the connections between follicular cells and oocytes in females, which may lead to a delay in ovarian development (42). In zebrafish, $HgCl_2$ also tends to bioaccumulate in the kidneys and has limited capacity to pass to blood-brain barriers (8).

1.3 Application of zebrafish Model to Environmental Toxicology

Danio rerio, commonly known as zebrafish is a freshwater fish that is mostly used in developmental biology and genetic studies but their use in toxicology, as well as in safety assessment, has been increasing (44). Zebrafish is also used in disease biology, behaviour (45) and is an emerging model for fertility research (46). It is also a good toxicological model

because many drugs and environmental pollutants have been reported from zebrafish experiments as having similar effects to ones in higher vertebrates, including humans (47).

Zebrafish embryos and larvae are good models to use for large drug-screening tests because of their permeability to many chemicals and drugs (48). They can absorb small molecules diluted in water by the skin and gills, larger molecules like proteins can be microinjected in the yolk sac, sinus venous or circulation system and/or enter for the mouth after 72 hours post-fertilization (hpf) (49). Moreover, zebrafish has a small generation time (3 to 6 months to maturation), easily bred, a large number of eggs per reproduction (500 to 600 eggs per week) and external fertilization with transparent eggs that allows the observation of the embryonic development (46).

Zebrafish is also a good model because it has a small size requiring small quantities of the testing products and generally few laboratory resources when compared with bigger animals (44). Additionally, other advantages of the use of zebrafish include the genome completely elucidated which helps to understand mechanisms in toxicology at a molecular level and 71.4% of human genes are similar to zebrafish genes (50).

In spite of these aspects, there are some disadvantages to the use of zebrafish for toxicological studies. First, compound metabolization in zebrafish may differ from mammals (51). Moreover, in early life stages (~ until 48 hpf), zebrafish has a protective membrane (chorion) that difficult the diffusion of some chemicals and non-water soluble chemicals cannot be easily dispersed (51).

1.4 Normal zebrafish development and reproduction

In adult zebrafish, the structure and function of gonads are similar to humans (52). In male zebrafish , there are paired testes with tubule organization (53). This organization has Sertoli cells that are present in the walls and support testes morphogenesis and spermatogenesis. Additionally, there are Leydig cells that are present in interstitial space and are the primary testosterone producers (54). The main difference between the male reproductive system in humans and zebrafish is in the Sertoli cells. In humans, these cells can be divided into two different stages separated by puberty. In fetal life, the Sertoli cells are responsible for the testis formation and sexual differentiation. That means that they are responsible for the testicular development, formation of seminiferous cord, prevention of germ-cells entry into meiosis, differentiation and function of Leydig cells and regression of

Muller ducts (they are present in embryos of both sexes but only in female they develop into reproductive organs (55)) through the secretion of anti-Mullerian hormone (56). In puberty, the maturation process of the Sertoli cells occurs and the capacity of proliferation is lost and inter-Sertoli cells tight junctions are formed and new functions appear (57). After maturation, these cells are responsible for spermatogenesis. They provide physic and metabolic support to germ-cell differentiation, meiosis, transformation into spermatozoa and the number of Sertoli cells is positively related to the number of spermatozoids (57). Zebrafish, instead of having a few germ cells with different development stages like men and many superior vertebrates, have a group of Sertoli cells that develop synchronously (58) and do not lose the capacity of proliferation over time (59). Male zebrafish has also an accessory sperm duct gland that serves mainly to secrete substances that are linked to the diverse mechanisms of sperm release and produce the sperm trails (54).

In wild, the mating is mainly in monsoon season although it is possible that females have mature ovum all year if food is available (60). The photoperiod is also very important, being the first hour of light the key for spawning events. Female zebrafish prefers to mate along shallow shorelines. In the lab, it is important to simulate the photoperiod, adding the appropriate amount of cold water to simulate the rain and provide a shallow surface to increase the number of eggs released. Basic mating behaviours include elliptical movements made by the male around the female (61). Males first release the sperm that will move in the water for several minutes and then females will release the eggs. After the females deposit the eggs, males start swimming next to the nest to accelerate sperm dispersal and mixing with the water, accelerating egg insemination (62).

Zebrafish has seven mainly embryonic development stages (Figure 2): zygote, cleavage, blastula, gastrula, segmentation, pharyngula, hatching and early larva period (63). The first period is the zygote, with about 700 μm of diameter and consists of the vitello plasm. The vitello plasm consists of the yolk globules and the ooplasm that contains numerous organelles. The ooplasm forms three interconnected domains: a blastodisc at the top of the animal hemisphere, a layer of ectoplasm at the yolk cell periphery, and a network of endoplasmic lacunae in the yolk cell (64). After the zygote period, the cleavage period began and the cell cycles occur rapidly and synchronously (63). Then, in the blastula period, cell cycles lengthen and become asynchronous during the mid-blastula transition. Cells at the blastoderm margin collapse into the yolk and form the yolk syncytial layer, a thin,

multinucleate structure at the interface of the blastoderm and the yolk and then the epiboly begins (65).

In the gastrula period, the future dorsoventral axis becomes obvious through asymmetry in the thickness of the blastoderm and is characterized by the movement of single cells rather than coherent cell layers. There is the formation of hypoblast and epiblast that converge from ventral and lateral positions toward the dorsal side. At the end of epiboly, the embryo extends along the dorsal side of the yolk sphere, with the head positioned at the former animal pole and the tailbud developing at the former vegetal pole of the egg (66).

The segmentation period is responsible for the development of somites, pharyngeal arch primordia, and neuromeres, primary organogenesis, earliest movements and the appears of the tail (63).

In the pharyngula period, the body axis straightens from its early curvature about the yolk sac; circulation, pigmentation, and tins begin development (63).

In the end, the hatching period completion of rapid morphogenesis of primary organ systems, the cartilage development in head and pectoral tin and hatching occur asynchronously and in the early larval period appears the swim bladder inflates, food-seeking and active avoidance behaviours (63).

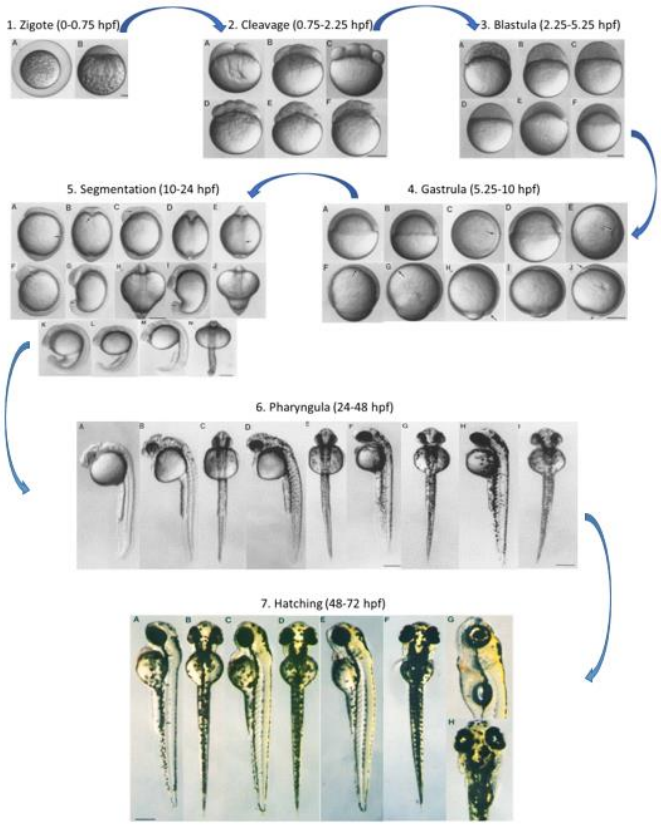

Figure 2: Zebrafish embryonic stages: ***1****. Zygote period with* ***A:*** *few mins after fertilization and* ***B:*** *about 10 min after fertilization;* ***2.*** *Cleavage period with* ***A****: 2-cell stage (0.75 h),* ***B****: 4-cell stage (1 h),* ***C****: 8-cell stage (1.25 h),* ***D****: 16-cell stage (1.5 h),* ***E****: 32-cell stage (1.75 h) and* ***F****: 64-cell stage(2 h);* ***3****. Blastula period with* ***A****: 256-cell stage (2.5 h),* ***B****: High stage (3.3 h),* ***C****: Transition between the high and oblong stages (3.5 h),* ***D****: Transition between the oblong and sphere stages (3.8 h),* ***E****: Dome stage (4.3 h) and* ***F****: 30%-epiboly stage (4.7 h);* ***4****. Gastrula period with* ***A****: 50%-epiboly stage (5.25 h),* ***B, C****: Germ ring stage (5.7 h),* ***D, E****: Shield stage (6 h). The embryonic shield, marking the dorsal side, is visible as a thickening of the germ ring to the left,* ***F****: 70%-epiboly stage (7.7 h). The dorsal side of the blastoderm, to the left, is thicker than the ventral side, to the right. The anterior axial hypoblast, or prechordal plate (arrow), extends nearly to the animal pole,* ***G****: 75%-epiboly stage (8 h). The arrow indicates the thin evacuation zone on the ventral side,* ***H, I****: 90%-epiboly stage (9 h). The tail bud (arrow) becomes visible in some embryos at this stage,* ***J****: Bud stage (10 h);* ***5.*** *Segmentation period with* ***A****: Two-somite stage (10.7 h). Somite 2 is the only one entirely pinched off at this time, the arrow indicates its posterior boundary. Somite 1 is just developing a clear anterior boundary at this stage,* ***B****: Two-somite stage, ventral view.* ***C, D****: Four-somite stage (11.3 h),* ***E****: Five-somite stage (1 1.7 h), ventral view, the focus is on the newly forming Kupffer's vesicle (arrow).* ***F****: Eight-somite stage (13 h). The optic primordium has a prominent horizontal crease (arrow),* ***G****: Thirteen-somite stage (15.5 h),* ***H****: Fourteen-somite stage (16 h), dorsal view, and positioned so that the first somite pair is at the center,* ***I, J****: Fifteen-somite stage (16.5 h). The arrow shows Kupffer's vesicle,* ***K****: Seventeen-somite stage (17.5 h),* ***L****: Twenty-somite stage (19 h). The arrow indicates the optic vesicle.* ***M****: Twenty-five-somite stage (21.5 h). The telencephalon is prominent dorsally, at the anterior end of the neuraxis.* ***N****: Twenty-five somite stage, dorsal view;* ***6****. Pharyngula period with: A: Left-side view at the prim-5 stage (24 h),* ***B, C****: The prim-1 2 stage (28 h),* ***D, E****: The prim-20 stage (33h),* ***F, G****: The prim-25 stage (36 h). Pigment extends almost to the end of the tail. The arrow in F indicates the ventral horn of melanophores.* ***H, I****: The high-pec stage (42 h). Pigment now extends the whole length of the embryo; 7. Hatching and early larva period with* ***A, B****: Long-pec stage (48 h),* ***C, D****: Pec-fin stage (60 h),* ***E, F****: Protruding-mouth stage (72 h),* ***G, H****: Early larva (120 h). Adapted from* (63).

1.5 Effects of Hg on Zebrafish development and reproduction

The toxicity of Hg on zebrafish depends on the stage of development, the dosage and time of exposure and can become irreversible and even lead to death (67). In zebrafish larvae (~6 days post fertilization, dpf), an exposure higher than 100 nM of $HgCl_2$ significantly increased mortality rate. Exposure between 7.5 to 100 nM, induced motor deficit, decreased swimming speed, elevated resting time and lake of response (8). Exposure to $HgCl_2$ also decreased body length and delayed the hatching period (68). Zebrafish larvae exposed to $HgCl_2$ also showed locomotor and biochemical defects in proteins, lipids, carbohydrates and nucleic acid levels that contributed to the behavioural impairment (8).

Exposure to Hg is related to dose-response motility parameters in zebrafish sperm and the effective concentrations are reduced in parallel with the exposure duration (69). Hg affected the physiology of spermatozoa and therefore, caused a decrease in fertilization success by injuring mitochondria, affecting water channels of the plasma membrane, displacing Ca^{2+} ions and inducing oxidative stress (69). In testis, sublethal exposure to MeHg chloride caused thickens of the tubule walls, probably resulting in inhibition of spermatogenesis and disorderly arranged spermatozoa which might be a signal of sperm necrosis (70). In the ovary, exposure to Hg caused degenerative changes such as atresia (follicular degeneration) and the loss of contact between the oocyte cell membranes and the follicular cell layer which might lead to delayed ovary development (70).

Exposure to Hg for 168 hpf induced oxidative stress affecting antioxidant enzyme activities, such as Catalase (CAT), Glutathione S-transferase (GST), Glutathione Peroxidase (GPx), Superoxide dismutase (SOD) (71). Exposure to Hg induced an increase in the CAT activity, indicating that an antioxidant status was increased to neutralize the oxidative stress (72). Moreover, Hg increased the GST activity, by increasing the formation of conjugates between Hg^{2+} and glutathione (GSH), indicating a protective and adaptative response. GPx decreased with exposure to Hg, indicating an increased utilization for the elimination of hydrogen peroxide (H_2O_2) and lipid hydroperoxides. Endogenous GSH increased with Hg exposure suggesting the enhanced GSH biosynthesis in an attempt to protect the fish from oxidative stress and lipid peroxidation (Malondialdehyde - MDA - contents) (72). All the above suggests that Hg exposure induced ROS generation and caused severe oxidative stress

as well as mRNA damage genes (cat1, sod1, gstr and gpx1a, that are transcriptional levels of genes encoding the antioxidant enzymes above) encoding antioxidant proteins (72).

1.6 Biomarkers response as a tool to assess Hg effects

Biomarkers may be defined as any biological response of varying nature (e.g. molecular, cellular or physiological) to a stressor, measured inside an organism or in its sub-products (e.g. urine, faeces, hair, feathers, etc.), indicating a stress-related deviation from the normal status of the individual to the stressor before direct components of fitness (e.g. survival) are affected (73). The assay to quantify biomarkers should be reliable, cheap and easy to perform. Baseline data of the biomarker should be well defined in order to distinguish between natural variability (noise) and contaminant-induced stress (signal) and the impacts of confounding factors to the biomarker response, the underlying mechanism of the relationships between biomarker response and pollutant exposure (dosage and time) and the toxicological significance of the biomarker should be well established (74).

According to the National Research Council (NRC) and WHO, there are 3 types of biomarkers (75,76):

- Biomarkers of effect – correspond to biochemical, physiological, behavioural or other alteration in an organism that, depending upon the magnitude, can be recognized as impairment or disease (77).
- Biomarkers of susceptibility – correspond to inherent and/or acquired ability of an organism to respond to the challenge of exposure to a specific xenobiotic substance (e.g. polymorphisms of detoxification systems) (78).
- Biomarkers of exposure – correspond to any contaminant, derived metabolites and/or interactive product between the contaminant compound and endogenous components of the cell, measured in the organisms' body fluids, internal tissues or another biological matrix (e.g. feather, urine, etc.) (75,76).

1.6.1 Oxidative stress markers

Oxidative stress has been described as a serious imbalance between the production of ROS and the antioxidant defences (79). ROS, in low amounts are essential to cells, but when

produced in a deregulated way they are an unavoidable by-product of metabolic processes of organisms, and can damage cell contents (e.g. proteins, lipids, DNA) which in turn may lead to cellular senescence and death (79,80). ROS include superoxide anion radical ($O_2^{\bullet -}$), hydroxyl radical ($OH^{\bullet}$), peroxyl radical ($RO_2^{\bullet}$), hydrogen peroxide (H_2O_2), etc. (79). CAT, GSH, GR and GST are some of the enzymes that help to maintain the redox status of cells and avoid oxidative stress. In Figure 3 there are represented the interaction between antioxidant enzymes present in the elimination of ROS. CAT eliminate ROS, converting H_2O_2 in water (H_2O) and molecular oxygen (O_2) (81). GST catalyses the transformation of a wide variety of electrophilic compounds to less toxic substances by conjugating them to GSH (82,83). In addition, some GST isozymes display peroxidase activity with respect to lipid hydroperoxide (LOOH) (84,85). GR reduces the glutathione disulfide (GSSG) in GSH (86).

Hg makes alterations in the antioxidant defence system and induces the production of ROS (87–89). Because Hg induces alterations in antioxidant enzymes such as CAT, GST, GSH, GR, etc., they are considered as biomarkers of Hg effect (90).

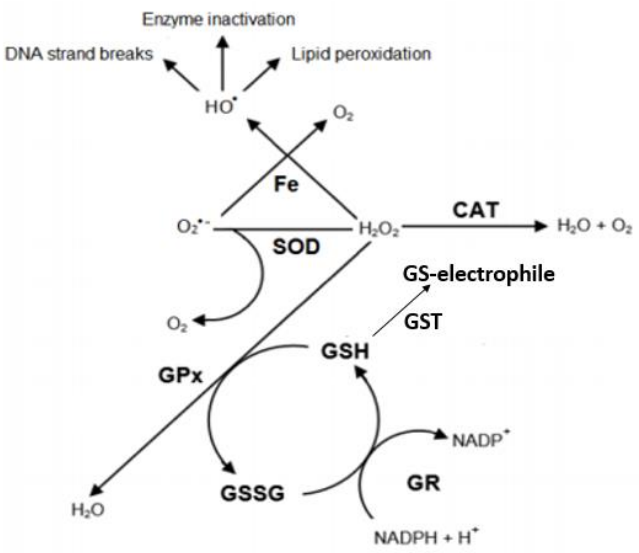

Figure 3: Representative diagram of the interaction between antioxidative enzymes. Adapted from (86,91)

1.6.2 Cholinesterase activity

Cholinesterase is a family of esterase enzymes responsible for hydrolysing the neurotransmitter acetylcholine into choline and acetic acid at synapses and neuro-effector

junctions (92). This family consists of two sister enzymes: acetylcholinesterase (AChE) which is presented in the nervous system and butyrylcholinesterase (BChE) which occur in serum and liver but the particular function of the enzyme remains undiscovered (92,93).

ChE activity has been traditionally used in environmental toxicology as a proxy for the exposure of organophosphate and carbamate pesticides (92). The competitive binding of the agonists to the active centre of acetylcholinesterase leads to the accumulation of acetylcholine within synaptic clefts and, thus, to an inactivation of signal transduction across cholinergic synapses (94). The inhibition of ChE activity can be used as a tool to evaluate the organism exposure to neurotoxic compounds such as metals (95,96).

Zebrafish only have the gene for AChE, which is responsible for the whole ACh degradation, being the BChE absent (97). AChE has already been identified, cloned and functionally detected in the zebrafish brain, so it is an important biomarker of effect for neurotoxicity studies and it is essential for neuronal and muscular development in zebrafish embryos (98).

1.6.3 Phosphoprotein phosphatase 1

Protein phosphatases (PPs) are a class of enzymes that remove the phosphate group from the phosphorylated amino acid residue and in turn, regulate the activity of their target phosphoproteins in cellular processes (99). The presence or absence of a phosphate group can change the conformation of the target protein, modifying its activity. Protein kinases (PK), other phosphoregulatory proteins, covalently attach a phosphate group to a target. Protein phosphorylation is implicated in many areas of cellular biology; such as transcriptional control, signal transduction, regulation of the cell cycle, immunoproliferation, development, apoptosis, and targeted proteolysis (99).

PPs can be divided into three classes based on the sequence, structure and catalytic function. Those classes are: a) serine-threonine protein phosphatases (STPPs), b) tyrosine phosphatases and c) dual-specific phosphatases that dephosphorylate all three residues (100). The STPPs are classified into three structurally unrelated families: phosphoprotein phosphatase (PPP), metallo-dependent protein phosphatases (PPM) and CTD aspartate-based protein phosphatases (FCP/SCP). The largest class of PPs is the PPP superfamily comprising PPP1, PPP2A, PPP2B, PPP4, PPP5, PPP6 and PPP7, differing only in their N- and C- terminus and sharing high homology in the catalytic domains (101–103). The

majority of phosphatase activity in eukaryotic cells belongs to PPPs, mainly to protein phosphatase 1 (PPP1) and protein phosphatase 2A (PPP2A) (104). PPP1 is involved in the regulation of several cellular events like glycogen metabolism, cell cycle, and sperm motility (105,106). In humans, the catalytic subunit is encoded by three different PPP1 genes (*PPP1CA*, *PPP1CB*, and *PPP1CC*), that give rise to four isoforms PPP1CA, PPP1CB, PPP1CC1, and PPP1CC2 and can bind to other non-catalytic subunits like PPP1 regulatory subunit that plays an important role in substrate specificity (107). The difference between the isoforms of PPP1C resides mainly in the C-terminal (108) (Figure 4).

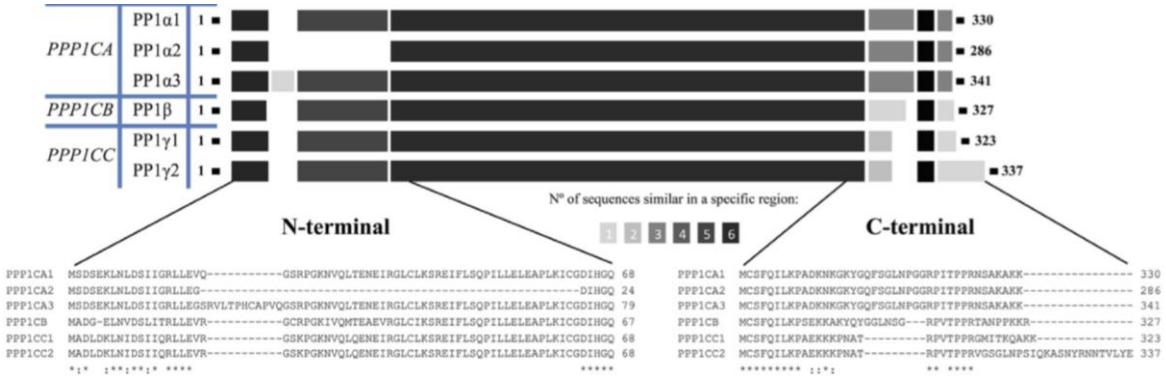

Figure 4: Schematics of all PPP1C isoform proteins. The bars represent the sequences and the scale of grays represent the similarity (1- no similarity, 6- high similarity) (100).

In humans, the PPP1CC2 is the isoform testis-enriched and sperm-specific (109). All four forms of PPP1C are expressed in mammalian testis (110), but PPP1CC2 is the isoform in higher amounts in testis and spermatozoa (111). PPP1CC2 is predominantly localized in post-meiotic cells, cytoplasm of secondary spermatocytes, round and elongated spermatids (108,110). In the spermatozoa, this isoform is distributed through the flagellum midpiece, and posterior region of the head suggested a role in motility and acrosome reaction. Moreover, decreased PPP1CC2 activity is associated with increased motility, so PPP1CC2 is thought to be a key protein for regulating sperm motility (108).

There are evidences that on zebrafish, PPP1 has five genes related to the mammalian genes PPP1CA, PPP1CB and PPP1CC. Two genes are similar to PPP1CA (ppp1caa and ppp1cab), two other genes are similar to PPP1CB (ppp1cb and ppp1cbl) and another gene is similar to PPP1CC (ppp1cc) (112).

2. Objectives and relevance of the study

We decided to study the effects of Hg exposure in zebrafish early development stage phases.

To accomplish the general goal of this study, the following specific aims were proposed:

1) To evaluate the survival and hatching rate of zebrafish as well as the morphological alterations during the exposure period;
2) To evaluate the effects of Hg on biomarkers of effect for neurotoxicity (AChE) and for oxidative stress (GST, GR, and CAT);
3) To study the effect of Hg on the expression of PPP1CC and GPx4.

Hg is one of the most toxic elements threatening the biosphere at large and humans in particular, with levels steadily rising due to both natural and human activities (113).

Zebrafish larvae is a good model to study the Hg effects in the early development stages of human life, because many drugs and environmental pollutants have been reported from zebrafish experiments as having similar effects to ones in higher vertebrates, including humans (47).

For this study, we selected three concentrations of Hg (0, 10 µg/L and 100 µg/L) in order to have control, the highest asymptomatic (10 µg/L - no visible deformations) and highest sub-lethal concentrations (100 µg/L).

To our knowledge there are no published results about the PPP1CC evolution in zebrafish, so we identify and analyze its expression for the first time in zebrafish embryonic development. For GPx4, there are only a few results available and they are about its expression in the first 24 hpf (114,115), so we monitor for the first time the expression of this proteins in the first 96 hpf of zebrafish development.

3. Material and Methods

3.1 Zebrafish husbandry and embryos collection

Adult zebrafish was maintained at the facility at the Department of Biology of University of Aveiro in a flow-through system with carbon-filtered water at 27.0 ± 1 °C with a 14:10 h photoperiod (light: dark) and fed twice a day with commercially available artificial diet. Conductivity was kept at 750 ± 50 μS/cm1, pH at 7.5 ± 0.5 and saturation of dissolved oxygen at 95%. These conditions were maintained in order to induce the reproductive cycle of fishes.

Zebrafish eggs were collected within 30 min after natural mating and rinsed in fish system water. Males and females were placed for crossing in aquariums (natural mating) as described in Andrade et al., (2016). Eggs were collected immediately after fertilization.

For fish mating, at the beginning of light cycle of the applied photoperiod, males and females were placed for crossing in aquariums (natural mating) with marbles on the bottom, to protect eggs from predation by adults. Eggs were collected 30 min after spawning, rinsed in system water and checked under a stereomicroscope (Stereoscopic Zoom Microscope - SMZ 1500, Nikon Corporation) for unfertilized or injured eggs. Eggs were separated and individual exposed to three different concentrations of $HgCl_2$ (C0=control, C1=10 μg/L and C2=100 μg/L) in 24-well plates for 96 h. Then, for each concentration, fertilized eggs were randomly transferred into Eppendorf's at 0 hpf, 24 hpf, 48 hpf, 72 hpf and 96 hpf, frozen in liquid nitrogen and stored at -80ºC for further analysis .

3.2 Morphological analyses

For each timepoint morphological analyses were carried out and five replicates of 10 eggs/larvae for biomarkers analyses and three replicates of 6 eggs/ larvae for Western Blot were collected. Morphological traits assessed were hatching delay, pigmentation, balance, tail deformation, curvature, pericardial edema and yolk absorption. These observations were according to Fish Embryo Acute Toxicity Test (FET) in OECD 236 Protocol (116). Each day, the eggs/larvae were transferred to Eppendorf's (one Eppendorf per replicate) and were frozen in liquid nitrogen and stored at -80ºC until analysis.

3.3 Biomarkers analysis

3.3.1 Sample preparation for biochemical analysis

To each sample previously prepared, 0.5 mL of K-phosphate buffer (0.1 M, pH = 7.2) was added and samples were homogenized at 4ºC using a U200S control IKA LABORTECHNIK. Following this, samples were centrifuged (10,000 g, 20 min, 4ºC), the obtained post-mitochondrial supernatant (PMS) was divided into different aliquots (two aliquots: 150 µl PMS; four aliquots: 50 µl PMS) and stored at -80ºC until biomarker analysis.

3.3.2 Protein determination

Protein concentration in samples was determined following the Bradford method (117). Briefly, in a 96-well microplate, 10 µL of sample was added in triplicate. A protein standard (concentrations: 0.0 mg/mL, 0.2 mg/mL, 0.5 mg/mL and 1.0 mg/mL) was prepared using a stock solution of bovine ɣ- globulin 1 mg/mL, added in quadruplicate in the microplate. Following this, 250 µL of a protein detection kit solution (Bio-Rad®) was added, the microplates were incubated at room temperature for 15 min, and the absorbance measured at 595 nm. A standard curve was obtained and used to determinate the total protein concentration of each sample.

All photometric measurements were carried out using a Multiskan Spectrum, reader (Thermo Scientific®).

3.3.3 Cholinesterase (ChE) activity

The activity of ChE was determined in triplicate, according to the Ellman's method (118) adapted to microplate by Guilhermino et al. (119). Briefly, 50 µl of sample and 250 µl of the reaction buffer were added to each well, the microplates were incubated at room temperature for 10 min, and the absorbance was measured at 414 (measurement times: 10, 15 and 20 min). The reaction buffer was a mixture of 1 ml of 5.50-dithiobis-2-nitrobenzoic acid solution (DTNB; 10 mM), 0.2 ml of acetylthiocholine solution (ASCh; 0.075 M) and 30 ml of K-phosphate buffer (0.1 M, pH=7.2). Enzymatic activity is expressed in nmol of substrate hydrolyzed per minute per mg of protein in PMS (nmol/min/mg of protein), using a molar extinction coefficient of $13.6x10^3$ M^{-1} cm^{-1}.

3.3.4 Catalase (CAT) activity

The CAT activity was determined in triplicate, following the Claiborne's method adapted to a UV microplate. Briefly, in a 96-well UV microplate, 20 µl of the sample, 130 µl K-Phosphate buffer (0.05 M, pH=7.0) and 150 µl of hydrogen peroxide (H_2O_2; 0.03 M) were added to each well. The absorbance was then immediately read at 240 nm, in 20 s intervals, for 3 min. The enzymatic activity presented is expressed as µmol of the substrate (H_2O_2) hydrolyzed per minute per mg of protein in PMS (µmol/min/mg of protein), using a molar extinction coefficient of 40 M^{-1} cm^{-1}.

3.3.5 Glutathione Reductase (GR) activity

GR activity was measured following the Cribb's method (120) adapted to microplate. Briefly, 20 µL of sample and 280 µL of the reaction buffer was added, in triplicate, and the absorbance was measured at 340 nm, in 20 s intervals, for 3 minutes. For the preparation of the reaction buffer, 17.2 mg of NADPH, 65.4 mg of glutathione disulfide (GSSG) and 19.6 mg of diethylenetriaminepentaacetic acid (DTPA) were dissolved in 100 mL of K-phosphate buffer (0.05 M, pH=7,0). Enzymatic activity is expressed as nmol of NADPH oxidized per minute per mg of protein in PMS (nmol/min/mg of protein), using a molar extinction coefficient of 6.22^3 M^{-1} cm^{-1}.

3.3.6 Glutathione s-transferase (GST) activity

GST activity was determined using the Habig's method (121), adapted to microplate (122). Briefly, 100 µl of sample and 200 µl of a reaction buffer were added in triplicate, and absorbance was measured at 340 nm, in 20s intervals, for 5 min. The reaction buffer was a mixture of 14.85 ml of K-phosphate buffer (0.1M, pH=6.5), 0.45 ml of 1-chloro-2,4-dinitrobenzene (CDNB; 10 mM) and 2.70 mL of glutathione reduced (GSH; 10 mM). Enzymatic activity is expressed as nmol of substrate (GSH) hydrolyzed per minute per mg of protein in PMS (nmol/min/mg of protein), using a molar extinction coefficient of 9.6×10^{-3} M cm^{-1}.

3.4 Analysis of protein expression

3.4.1 Preparation of zebrafish lysate

To prepare zebrafish embryo protein extracts, the three replicates with 6 eggs each were homogenized with SDS 1% (5 µL per egg). Tubes were maintained on constant shack at 4ºC for 30 min and then centrifuged at 16,000 x g for 20 min at 4ºC. Then the tubes were gently removed from the centrifuge and placed on ice. The supernatant was transferred to new fresh tubes kept on ice until protein quantification and the pellets were frozen.

3.4.2 BCA assay protocol for Western Blot

The protein content of the samples was determined using the Pierce bicinchoninic acid (BCA) Protein Assay Reagent Kit (Fisher Scientific, Loures, Portugal). Standard protein quantification was prepared as described in Supplementary Table 2. Samples were prepared by adding 6 µL sample in 54 µL lysis buffer. In a 96-well plate, 25 µL of each standard and sample were transferred in duplicate. The Working Solution (WS) was prepared by mixing BCA reagent A with BCA reagent B in the proportion of 50:1. Then, 200 µL of WS were added to each well, for standards and samples and incubated in the dark at 37ºC for 30 min. The absorbance was measured at 562 nm using an Infinite® 200 PRO (Tecan, Switzerland). A standard curve was obtained by plotting BSA standard absorbance vs BSA concentration and used to determinate the total protein concentration of each sample.

3.4.3 Western Blotting

The protein extracts of zebrafish embryos (with 30 µg of protein) were resolved by 15% SDS-polyacrylamide gel electrophoresis (PAGE) prepared as described in Supplementary Table 1 and proteins were transferred onto nitrocellulose membranes.

The gel was run at 200 V and transferred at 200 mA for 2h. After the transfer, the membranes were washed with 1x Tris Buffered Saline and Tween-20 (TBS-T). Then, the membrane was incubated with Ponceau Staining on a shaker for 5 minutes. The membrane was then washed with distilled water until the proteins were well defined and scanned.

For PPP1CC, the membrane were blocked with 5% non-fat milk in TBST 1X for 1h with agitation, washed in TBST 1X, incubated with primary antibody (anti-PPP1CC in 5% non-fat milk in TBST 1X in a dilution of 1:1000) for two hours at room temperature, washed

three times in TBST 1X for 10 min with agitation, incubated with secondary antibody (anti-rabbit in 5% non-fat milk in TBST 1X in a dilution of 1:10000) for one hour at room temperature, washed two times with TBST 1X for 10 min and once with TBS 1X with agitation and revealed in odyssey.

For GPx4, the membrane were blocked with 5% BSA in TBST 1X for 1h with agitation, washed in TBST 1X, incubated with primary antibody (anti-GPx4 in 5% BSA in TBST 1X in a dilution of 1:1000) for one hour at room temperature, washed three times in TBST 1X for 10 min with agitation, incubated with secondary antibody (anti-rabbit in 5% BSA in TBST 1X in a dilution of 1:5000) for one hour at room temperature, washed two times with TBST 1X for 10 min and once with TBS 1X with agitation and revealed in odyssey.

The image of the total protein (scanned with Ponceau) and the image of PPP1CC and GPx4 (odyssey) were treated and the bands were quantified in image Lab program. A ratio of PPP1CC : protein and GPx4 : protein were calculated and then statistical analysis were performed.

3.5 Statistical analyses

A series of two-way ANOVAs (analysis of variance) was used to test the effects of exposure time and Hg concentration on AChE, CAT, GR and GST activity. The Tukey HSD post-hoc test was applied (where ANOVA allowed it) to identify the homogeneous groups. The same techniques were also used to test the effects of time and Hg concentration on PPP1CC and GPx4 levels, For the abnormal development observed a one-way ANOVA was performed with the Dunnet post-hoc test. All analyses were carried out using SigmaPlot® 11.0 software (Systat Software Inc.).

4. Results

4.1 Impact of Hg exposure on zebrafish Morphology

Zebrafish were exposed to different $HgCl_2$ concentrations during different time periods. Our results show that eggs in the control group presented normal embryonic development and mortality remained below 10% throughout the experiment, validating the criteria of the OECD 236 protocol (Figure 5). At 24 hpf all the eggs were alive. After 48 hpf in the control group, 1.2% of the eggs hatched, in the group with 10 µg/L of Hg 2.2% hatched and 5.6% didn't survived, at 100 µg/L of Hg 7.8% of the embryos died and there was no hatching. At 72 hpf in the control group all had hatching and 1.2% of the larvae had died, at 10 µg/L of Hg all had hatching and at 100 µg/L of Hg 37.8% had hatching and 1.1% of the larvae died. In the end of the exposure, at 96 hpf, in the group with 100 µg/L of Hg, 65.6% had hatching, having yet 25.6% of embryos. The final percentage of mortality were 1.2% in control, 5.6% with 10 µg/L of Hg and 8.9% with 100 µg/L of Hg.

Figure 5: Percentage of zebrafish survival after Hg exposure.

In the Figure 6 there are represented the observed morphological malformations on the zebrafish larvae at 96 hpf after exposure to 0, 10 and 100 µg/L of Hg. In the left of the figure is demonstrated a normal larvae, in the middle is a larvae with a tail deformation and in the right a larvae with several defects (e.g. curvature, low yolk sac absorption and pericardial edema).

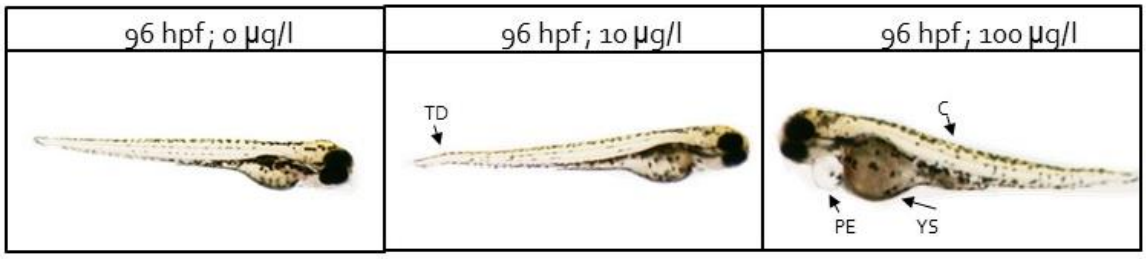

Figure 6: Observed morphological malformations at 96 hpf in different concentrations of Hg. TD – tail deformation; YS – low yolk sac absorption; PE – pericardial edema; C – curvature.

In Figure 7, is represented the average of abnormal development per animal exposed to Hg. The abnormal development of zebrafish embryos increases with the increase in Hg concentration. At 96 hpf, in average 1 larvea have 0.08 deformations in control, have 0.03 deformations with 10 µg/L of Hg, and 2.9 deformations with 100 µg/L of Hg, in percentage of abnormal development were 1.5%,.0.6% and 51.1% respectively.

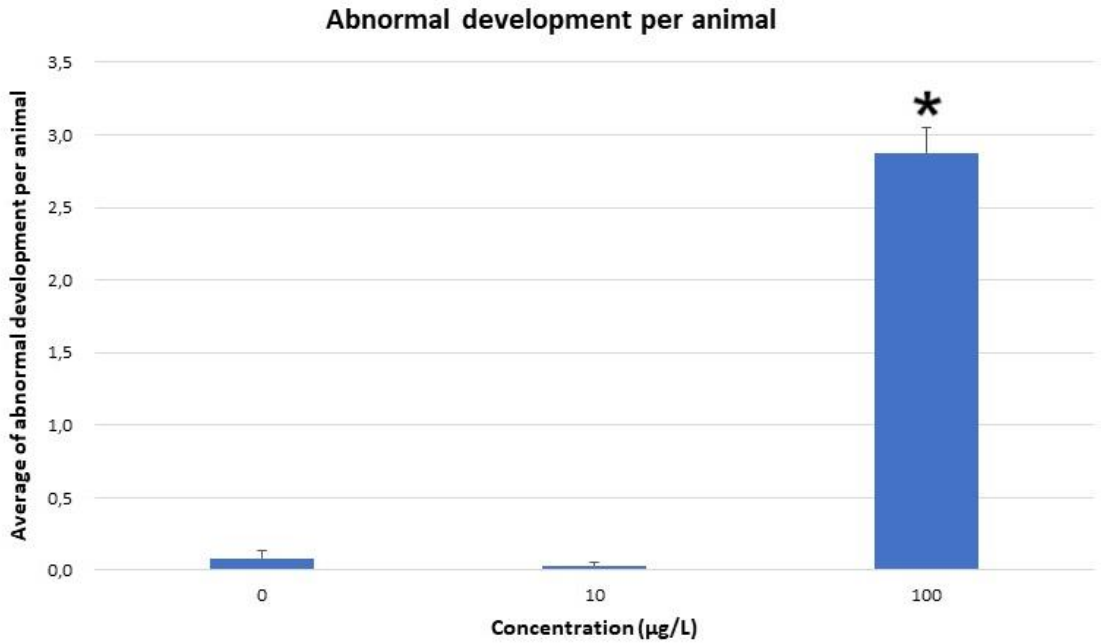

Figure 7: *Average of abnormal development per fish, on zebrafish after 96 hours of exposure to Hg. Data are expressed as mean ± SE; asterisks indicate significant different concentration compared with control (*- one-way ANOVA, post hoc: Dunnett test, $p < 0.05$)*

In Figure 8, is represented the abnormal development observed at 96 hpf. Only in the highest concentration tested there were significant abnormal development. The abnormal development more represented was the low equilibrium of the fish (67%), followed by curvature (61%), pericardial edema and low yolk sac absorption were next (52 and 52% respectively), followed by tail deformation (43%) and alteration in pigmentation (11%).

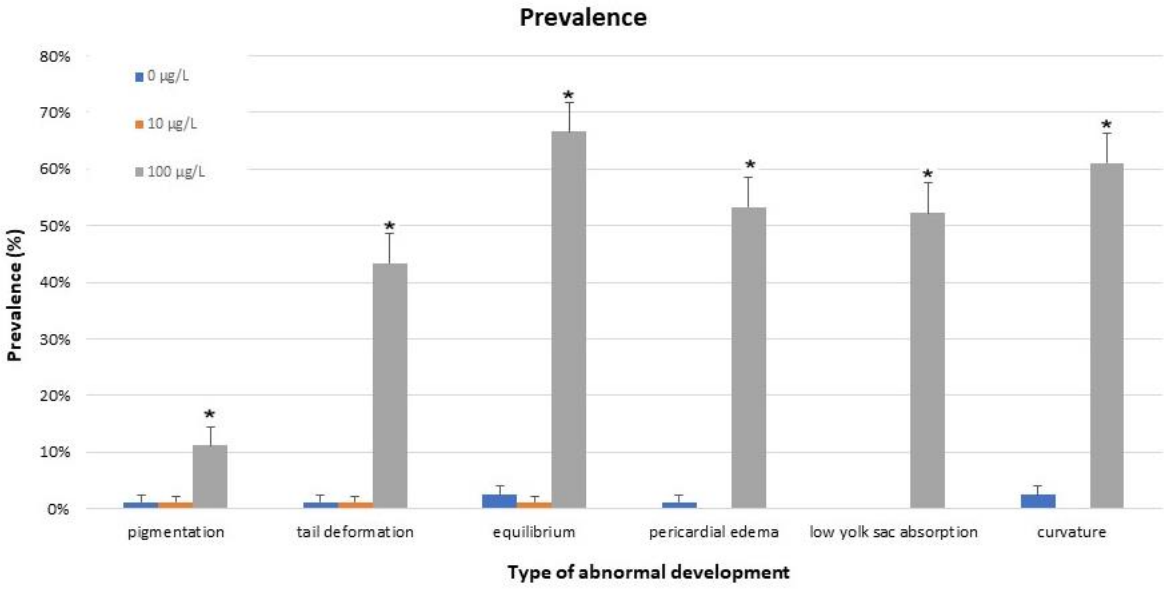

Figure 8: *Percentage of prevalence of each abnormal development on zebrafish after 96 hours of exposure to Hg. Data are expressed as mean ± SE; asterisks indicate significant different concentration compared with control (*- one-way ANOVA, post hoc: Dunnett test, $p < 0.05$)*

4.2 Impact of Hg exposure on biomarkers of effect

The Figure 9 indicate the results of ChE, CAT, GR and GST activities. ChE activity (in nmol/min/mg of prot) is inhibited by the highest concentration of Hg (100 µg/L) at 72 and 96 hpf. CAT activity (in µmol/min/mg of prot) is not significantly affected by the exposure to Hg although it has a tendency to decrease. GR activity (in nmol/min/mg of prot) increase at 48 hpf in both treatments (10 and 100 µg/L of Hg) and decrease at 72 hpf also in both treatments. GST activity (in nmol/min/mg of prot) increases with time, mostly since 48 hpf. At 48 hpf only the high concentration (100 µg/L) significantly increases and at 72 and 96 hpf there are an increase of activity in both concentrations (10 and 100 µg/L of Hg).

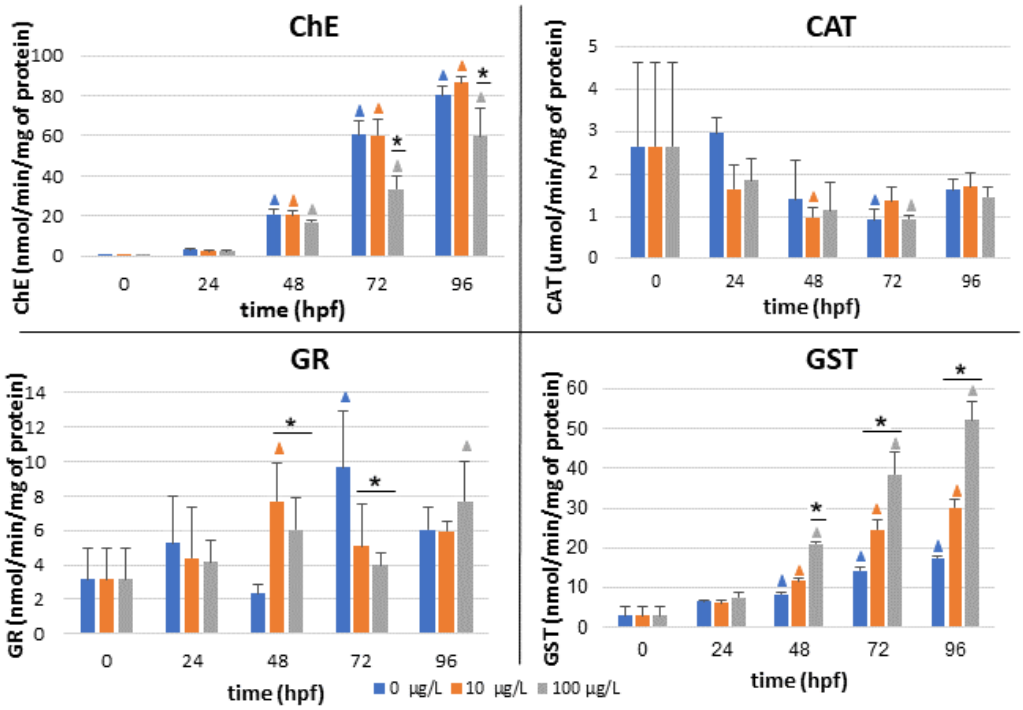

Figure 9: Levels of activity of ChE (nmol/min/mg of prot), CAT (µmol/min/mg of prot), GR (nmol/min/mg of prot) and GST (nmol/min/mg of prot) with different concentrations of Hg over time. Results were expressed as mean ± SE; "" indicates at each time point, significant differences with the respective control and "▲" indicates at each concentration (blue for 0 µg/L, orange for 10 µg/L and gray for 100 µg/L), significant differences with time 0 (two-way ANOVA, post hoc: Tukey test, $p < 0.05$).*

4.3 Protein expression analysis

4.3.1 PPP1CC expression

The UniProt website provides a multiple sequence alignment tool for proteins called 'Align' (123). Using this tool, we found areas of similarity between PPP1CC in zebrafish and PPP1CC1 and PPP1CC2 in human. To execute the multiple sequence alignment, we introduced the Uniprot identifiers (P36873-1 for human PPP1CC1, P36873-2 for human PPP1CC2 and A0A0R4IZT6-1 for zebrafish PPP1CC) into the sequence input box provided. The UniProt Align results are in Figure 10. These results showed that zebrafish PPP1CC and human PPP1CC1 have 316 identical positions, 6 similar positions and 97.833% of identity. Regarding the comparison between zebrafish PPP1CC and human PPP1CC2 we found that these proteins have 309 identical positions, 6 similar positions and 91.691% of identity.

```
A0A0R4IZT6 A0A0R4IZT6_DANRE   1   MADIDKLNIDSIIQRLLEVRGSKPGKNVQLQENEIRGLCLKSREIFLSQPILLELEAPLK   60
P36873     PP1G_HUMAN         1   MADLDKLNIDSIIQRLLEVRGSKPGKNVQLQENEIRGLCLKSREIFLSQPILLELEAPLK   60
P36873-2   PP1G_HUMAN         1   MADLDKLNIDSIIQRLLEVRGSKPGKNVQLQENEIRGLCLKSREIFLSQPILLELEAPLK   60
                                  ***:**********************************************************

A0A0R4IZT6 A0A0R4IZT6_DANRE  61   ICGDIHGQYYDLLRLFEYGGYPPESNYLFLGDYVDRGKQSLETICLLLAYKIKYPENFFL  120
P36873     PP1G_HUMAN        61   ICGDIHGQYYDLLRLFEYGGFPPESNYLFLGDYVDRGKQSLETICLLLAYKIKYPENFFL  120
P36873-2   PP1G_HUMAN        61   ICGDIHGQYYDLLRLFEYGGFPPESNYLFLGDYVDRGKQSLETICLLLAYKIKYPENFFL  120
                                  ********************:***************************************

A0A0R4IZT6 A0A0R4IZT6_DANRE 121   LRGNHECASINRIYGFYDECRRRYNIKLWKTFTDCFNCLPIAAIVDEKIFCCHGGLSPDL  180
P36873     PP1G_HUMAN       121   LRGNHECASINRIYGFYDECKRRYNIKLWKTFTDCFNCLPIAAIVDEKIFCCHGGLSPDL  180
P36873-2   PP1G_HUMAN       121   LRGNHECASINRIYGFYDECKRRYNIKLWKTFTDCFNCLPIAAIVDEKIFCCHGGLSPDL  180
                                  ********************:***************************************

A0A0R4IZT6 A0A0R4IZT6_DANRE 181   QSMEQIRRIMRPTDVPDQGLLCDLLWSDPDKDVLGWGENDRGVSFTFGAEVVAKFLHKHD  240
P36873     PP1G_HUMAN       181   QSMEQIRRIMRPTDVPDQGLLCDLLWSDPDKDVLGWGENDRGVSFTFGAEVVAKFLHKHD  240
P36873-2   PP1G_HUMAN       181   QSMEQIRRIMRPTDVPDQGLLCDLLWSDPDKDVLGWGENDRGVSFTFGAEVVAKFLHKHD  240
                                  ************************************************************

A0A0R4IZT6 A0A0R4IZT6_DANRE 241   LDLICRAHQVVEDGYEFFAKRQLVTLFSAPNYCGEFDNAGAMMSVDETLMCSFQILKPAE  300
P36873     PP1G_HUMAN       241   LDLICRAHQVVEDGYEFFAKRQLVTLFSAPNYCGEFDNAGAMMSVDETLMCSFQILKPAE  300
P36873-2   PP1G_HUMAN       241   LDLICRAHQVVEDGYEFFAKRQLVTLFSAPNYCGEFDNAGAMMSVDETLMCSFQILKPAE  300
                                  ************************************************************

A0A0R4IZT6 A0A0R4IZT6_DANRE 301   KKKPNPSRPVTPPRNMVTKQAKK--------------                         323
P36873     PP1G_HUMAN       301   KKKPNATRPVTPPRGMITKQAKK--------------                         323
P36873-2   PP1G_HUMAN       301   KKKPNATRPVTPPRVASGLNPSIQKASNYRNNTVLYE                         337
                                  ***** :*******     : .
```

Figure 10: "Align" results between PPP1CC in zebrafish and PPP1CC1 and PPP1CC2 in human.

Figure 11 shows the expression of PPP1CC during zebrafish development. These results demonstrate that PPP1CC protein content increases over time, but with different concentrations of Hg there are no statistically significant differences. We also can observe that with 100 µg/L of Hg there is a delay in the increase of PPP1CC until 72 hpf.

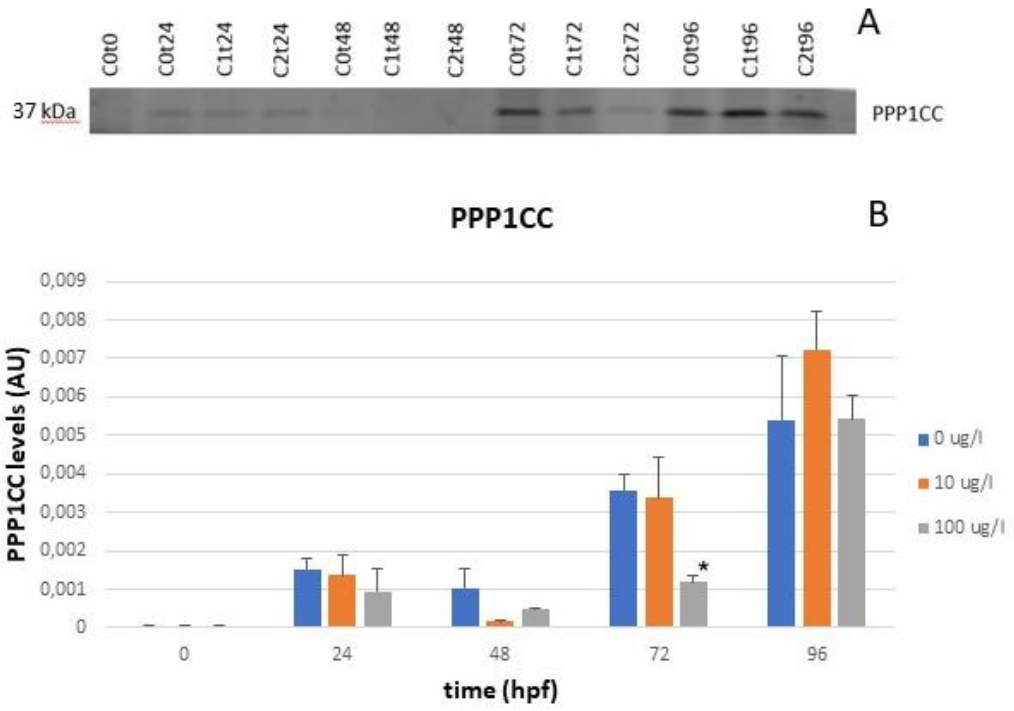

Figure 11: Impact of the Hg exposure on PPP1CC by Western blotting. A – Zebrafish embryos extracts were run on SDS-PAGE gels. Three different concentrations (C0=0 µg/L, C1=10 µg/L and C2=100 µg/L) of Hg were tested over time (t0 to t96 hpf). B - Protein expression was found to significantly increase ($p \leq 0.05$) with time. There were no statistically

significant differences between concentrations (p=0.130) or between time and concentration (p=0.320) except for a marginal (p=0.049) identification at 100 µg/L at the 72hpf. Data were expressed as mean ± SE. (n=3)

4.3.2 GPx4 expression

GPx4 expression (Figure 12) was not affect by time of exposure (p=0.259) nor by concentration of Hg (p=0.832). These results should be repeated since the bands in the membrane are too weak, and thus difficult to quantify.

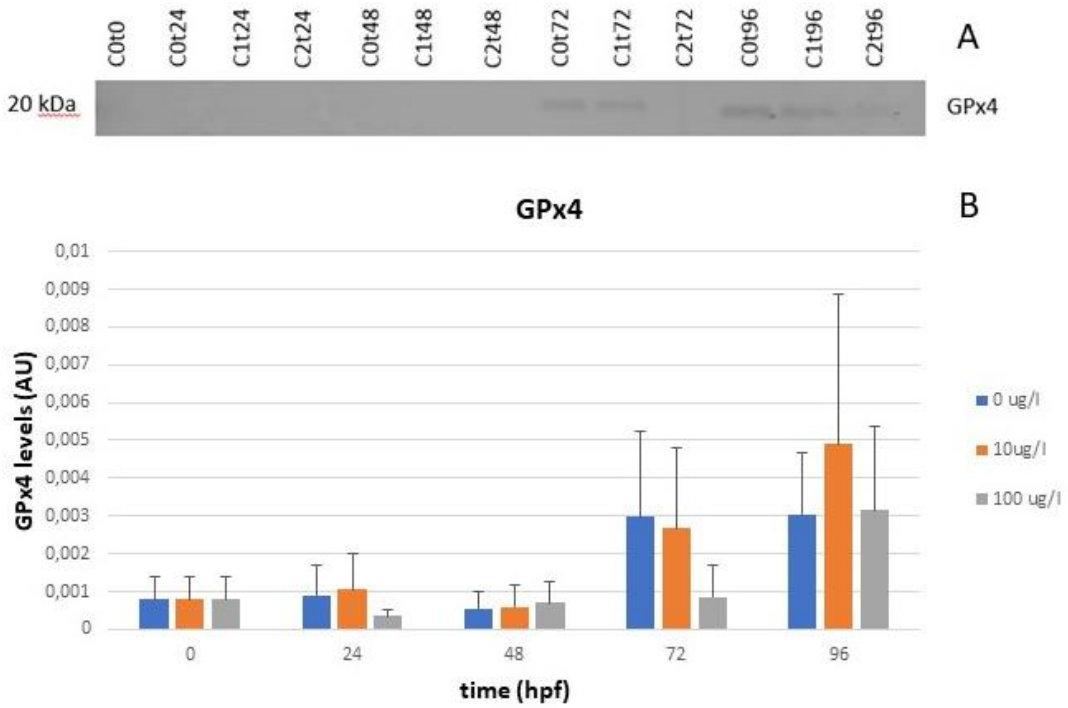

Figure 12: The immunoblotting in zebrafish with anti-GPx4 antibody showed the expression of GPx4 with three different concentrations (C0=0 ug/l, C1=10ug/l and C2=100 ug/l) of Hg over time (t0 to t96 hpf). There weren't statistical differences in time (p=0.259), in concentration (p=0.832) or between time and concentration (p=0.974). Data were expressed as mean ± SE. (n=3)

5. Discussion

5.1 Morphology

In the present study, high concentrations of Hg exposure (100 μg/L) decreased the hatching rate, delayed the hatching period and resulted in several non-lethal morphological abnormalities (equilibrium, curvature, pericardial edema, low yolk sac absorption, tail deformation and pigmentation), reflecting the developmental toxicity of Hg in zebrafish. Like our findings, Hg was reported to prolong the hatching time of other fishes (70,124,125). This delayed effect was probably caused by the inhibition of mitoses or suppression of embryogenesis (126,127), or by the inability of the emerging larvae to break the egg membrane (71). Reduced hatching success of Hg-exposed embryos was probably due to structural and functional disturbances during embryonic development (127). In our results we find that the equilibrium is the abnormal development most affected by Hg (67%) exposure probably duo to neurological effects (AChE) followed by curvature and tail deformations (61 and 43% respectively).

5.2 Neurotoxicity and oxidative stress biomarkers

Cholinesterase activity was measured to observe if there were some neurotoxic effects in zebrafish when exposed to Hg. AChE is the only cholinesterase present in zebrafish, so the results showed an increase of AChE activity over time. The exposure to Hg at high concentrations decreased AChE activity between 48 and 96 hpf with statistically significance. Similar concentrations of Hg were tested *in vitro* on the zebrafish and the result also suggests a decrease in AChE activity (97). As we refer previously, AChE it is an important biomarker of effect for neurotoxicity studies and it is essential for neuronal and muscular development in zebrafish embryos (98), so the inhibition of AChE can be related with the lack of equilibrium that we observed in the morphological analyses.

To assess potential effects of Hg exposure in oxidative stress of zebrafish, the activity of CAT, GR and GST in eggs and larvae were determined. CAT is responsible for the subsequent degradation of H_2O_2, generating non-toxic H_2O and is considered to be the first line defenses that directly scavenge ROS (50). In literature, exposure to Hg induced an increase in the CAT activity in brain and ovary, indicating an increase of the antioxidant status to neutralize the oxidative stress and decrease in liver indicating that the liver was not able to eliminate or neutralize the excess of ROS, decreasing enzyme activities or even

degrade the enzymes (50). In our study, CAT activity didn't change significantly between concentrations of Hg.

To maintain the redox status of the cells and avoid oxidative stress, glutathione reductase reduces the glutathione disulphide in GSH (86). We observe an increase of GR activity at 48hpf of Hg exposure indicating that the antioxidant status is neutralizing the oxidative stress, and a decrease of GR activity at 72 hpf indicating that the fish in not able to eliminate or neutralize more ROS. At 96 hpf there are no significant differences with the control. Studies show an increase in GR activity in zebrafish after 30 days of exposure (128).

GST activity was statistically significant higher in the presence of Hg in both concentrations (10 and 100 μg/L) after 72 and 48 hpf respectively. The increased GST activity upon Hg exposure could indicate a protective and adaptative response to Hg accumulation by elevating GST activity to increase the formation of conjugates between Hg^{2+} and GSH (129).

Hg can cross the blood brain barrier and accumulate in the brain, promoting the generation of oxidative stress and alterations in the metabolism of some proteins associated with the development of neurodegenerative diseases (97) so, probably, the oxidative stress induced by Hg treatment in zebrafish may be involved with the inhibitory effect observed on AChE activity.

5.3 Protein expression levels

We study for the first time the expression of PPP1CC in early development of zebrafish. PPP1CC has a high percentage of identity with PPP1CC1 and PPP1CC2 in human (97.833% and 91.692% respectively) but is closer of PPP1CC1. In human, PPP1CC1 is ubiquitous in somatic cells while PPP1CC2 is expressed in testicular germ cells and sperm (130). We showed that PPP1CC expression increase during the development of zebrafish embryos. Studies in mice testis showed that there is an increase of expression over time of development (108,110). PPP1CC expression decrease only at 72 hpf in the hight concentration of Hg.

GPx4 is a monomeric selenoenzyme harboring a selenocysteine in the catalytically active center (131). GPx4 plays various roles in controlling the cellular redox status (131), signal transduction, inflammation, and apoptosis (132). The loss of GPx4 activity has been linked to human diseases such as male infertility, arteriosclerosis, Alzheimer's disease and

Parkinson's disease (133). We decided to study this protein because little is known about its function and expression on fish. Two forms of GPx4 (GPx4a and GPx4b) have been identified in zebrafish, and their expression has been followed during embryonic development (134). Our study suggests that GPx4 expression is not affected neither for the time of development of the fish (0 to 96 hpf) nor for the exposure to mercury (control to 100 μg/L).

6. Conclusion

With this work, we wanted to test the effect of mercury in zebrafish early development. For that, we analyzed the effect of exposure to several concentrations of $HgCl_2$ on zebrafish morphology, selected protein expression (PPP1CC and GPx4), oxidative stress biomarkers (CAT, GST, and GR) and neurotoxic effect biomarkers (AChE).

Our study showed that high concentrations of Hg delay the hatching process and induce malformations mainly causing difficulties in equilibrium and curvature.

Exposure to Hg also induced alterations of the biomarker's levels (inhibit AChE after 72 hpf, promote GST after 48 hpf and GR activity is promoted at 48 hpf and inhibit as 72 hpf).

PPP1CC was for the first time identified in zebrafish and we saw an increase of expression with time. PPP1CC was only affected by mercury at 72 hpf in the highest concentration.

We did not find any significant alteration in protein expression of GPx4 or in CAT activity.

More studies are necessary to clarify the effect of mercury in zebrafish development and about expression of PPP1CC and GPx4 in zebrafish.

It seems also particular interesting to investigating if:

- Hg affects zebrafish over longer exposure times;
- the alterations provoked by mercury are reversible or not;
- the future generations have any inherited morphological, behaviour or enzymatical alterations.

References

1. Bailon MX, David AS, Park Y, Kim E, Hong Y. Total mercury, methyl mercury, and heavy metal concentrations in Hyeongsan River and its tributaries in Pohang city , South Korea. Environ Monit Assess. 2018;190(5):1–16.
2. World Health Organization. Mercury and health. 2017 [cited 2019 Feb 13].
3. Connor DO, Hou D, Sik Y, Mulder J, Duan L, Wu Q, et al. Mercury speciation, transformation, and transportation in soils, atmospheric flux, and implications for risk management: A critical review. Environ Int. 2019;126:747–61.
4. Pirrone N, Cinnirella S, Feng X, Finkelman RB, Friedli HR, Leaner J, et al. Global mercury emissions to the atmosphere from anthropogenic and natural sources. Atmos Chem Phys. 2010;10(13):5951–64.
5. Eagles-Smith CA, Silbergeld EK, Basu N, Bustamante P, Diaz-Barriga F, Hopkins WA, et al. Modulators of mercury risk to wildlife and humans in the context of rapid global change. Ambio. 2018;47(2):170–97.
6. Krabbenhoft DP, Sunderland EM. Global change and mercury. Science (80-). 2013;341(6153):1457–8.
7. Crook J, Mousavi A. The chlor-alkali process: A review of history and pollution. Environ Forensics. 2016;17(3):211–7.
8. Abu Bakar N, Mohd Sata NSA, Ramlan NF, Wan Ibrahim WN, Zulkifli SZ, Che Abdullah CA, et al. Evaluation of the neurotoxic effects of chronic embryonic exposure with inorganic mercury on motor and anxiety-like responses in zebrafish (*Danio rerio*) larvae. Neurotoxicol Teratol. 2017;59:53–61.
9. Sakamoto M, Itai T, Murata K. Effects of Prenatal Methylmercury Exposure: From Minamata Disease to Environmental Health Studies. Nihon Eiseigaku Zasshi. 2017;72(3):140–8.
10. Wikipedians B. Chemical Elements [Internet]. PediaPress; 710-731 p. Available from: https://books.google.pt/books?id=s1fWm6vpCMkC
11. Pacyna EG, Pacyna JM, Sundseth K, Munthe J, Kindbom K, Wilson S, et al. Global emission of mercury to the atmosphere from anthropogenic sources in 2005 and projections to 2020. Atmos Environ. 2010;44(20):2487–99.
12. ENVIRONMENT D. Ratification and Implementation of the Minamata Convention on Mercury. European commission. 2015. p. 5–6.
13. Environment DG. EU RULES ON MERCURY IN ACTION Reducing use and emissions of mercury. p. 4–5.
14. Gonzalez-Raymat H, Liu G, Liriano C, Li Y, Yin Y, Shi J, et al. Elemental mercury: Its

unique properties affect its behavior and fate in the environment. Environ Pollut. 2017;229:69–86.

15. Ariya PA, Amyot M, Dastoor A, Deeds D, Feinberg A, Kos G, et al. Mercury Physicochemical and Biogeochemical Transformation in the Atmosphere and at Atmospheric Interfaces: A Review and Future Directions. Chem Rev. 2015;115(10):3760–802.
16. Bargagli R. Moss and lichen biomonitoring of atmospheric mercury: A review. Sci Total Environ. 2016;572:216–31.
17. El-Safty SA, Shenashen MA. Organic – Inorganic Mesoporous Monolithic Scaffolds and Their Functionality in the Optical Ion -Sensitive Removal of Mercury Ions. 2013;
18. Engstrom DR. Fish respond when the mercury rises. Proc Natl Acad Sci U S A. 2007;104(42):16394–5.
19. Singh R, Gautam N, Mishra A, Gupta R. Heavy metals and living systems: An overview. Indian J Pharmacol. 2011;43(3):246–53.
20. Bhat SA, Hassan T, Majid S. Heavy metal toxicity and their harmful effects on living organisms – A REVIEW. Int J Med Sci Diagnosis Res. 2019;3(1):106–22.
21. Paige Wright L, Zhang L, Cheng I, Aherne J, R. Wentworth G. Impacts and Effects Indicators of Atmospheric Deposition of Major Pollutants to Various Ecosystems - A Review. Aerosol Air Qual Res. 2018;18:1953–92.
22. Ruszkiewicz JA, Teixeira de Macedo G, Miranda-Vizuete A, Bowman AB, Bornhorst J, Schwerdtle T, et al. Sex-Specific Response of Caenorhabditis elegans to Methylmercury Toxicity. Neurotox Res. 2018;(October).
23. Wolfe MF, Schwarzbach S, Sulaiman RA. Effects of mercury on wildlife: A comprehensive review. Environ Toxicol Chem. 1998;17(2):146–60.
24. Chan HM, Scheuhammer AM, Ferran A, Loupelle C, Holloway J, Weech S. Impacts of mercury on freshwater fish-eating wildlife and humans. Hum Ecol Risk Assess. 2003;9(4):867–83.
25. Pereira ME, Lillebø AI, Pato P, Válega M, Coelho JP, Lopes CB, et al. Mercury pollution in Ria de Aveiro (Portugal): A review of the system assessment. Environ Monit Assess. 2009;155(1–4):39–49.
26. Cachada A, Pereira ME, Ferreira Da Silva E, Duarte AC. Sources of potentially toxic elements and organic pollutants in an urban area subjected to an industrial impact. Environ Monit Assess. 2012;184(1):15–32.
27. Frederick P, Jayasena N. Altered pairing behaviour and reproductive success in white ibises exposed to environmentally relevant concentrations of methylmercury. Proc R Soc B Biol

Sci. 2011;278:1851–7.
28. Kobiela ME, Cristol DA, Swaddle JP. Risk-taking behaviours in zebra finches affected by mercury exposure. Anim Behav. 2015;103:153–60.
29. Maqbool F, Niaz K, Hassan FI, Khan F, Abdollahi M. Immunotoxicity of Mercury: Pathological and Toxicological Effects. J Environ Sci Heal Part C. 2017;35(1):29–46.
30. Wirth JJ, Mijal RS, Wirth JJ. Adverse Effects of Low Level Heavy Metal Exposure on Male Reproductive Function. Syst Biol Reprod Med. 2010;56(2):147–67.
31. Henriques MC, Loureiro S, Fardilha M, Herdeiro MT. Exposure to mercury and human reproductive health : A systematic review. Reprod Toxicol. 2019;85:93–103.
32. Mínguez-Alarcón L, Afeiche MC, Williams PL, Arvizu M, Tanrikut C, Amarasiriwardena CJ, et al. Hair mercury (Hg) levels, fish consumption and semen parameters among men attending a fertility center. Int J Hyg Environ Health. 2018;221(2):174–82.
33. Silva DAF, Teixeira CT, Scarano WR, Paula A, Favareto A, Fernandez CDB, et al. Effects of methylmercury on male reproductive functions in Wistar rats. Reprod Toxicol. 2011;31(4):431–9.
34. Kostic TS, Andric SA, Maric D, Kovacevic RZ. Inhibitory effects of stress-activated nitric oxide on antioxidant enzymes and testicular steroidogenesis. J Steroid Biochem Mol Biol. 2000;(75):299–306.
35. Debnath D, Mandal TK. Study of Quinalphos (an Environmental Oestrogenic Insecticide) Formulation (Ekalux 25 E . C .) -induced Damage of the Testicular Tissues and Antioxidant Defence Systems in Sprague-Dawley Albino Rats. J Appl Toxicol. 2000;(20):197–204.
36. Boujbiha MAM, Hamden K, Guermazi F, Bouslama A, Omezzine A, Feki A El. Impairment of Spermatogenesis in Rats by Mercuric Chloride : Involvement of Low 17 β - Estradiol Level in Induction of Acute Oxidative Stress. Biol Trace Elem Res. 2011;(142):598–610.
37. Homma-takeda S, Kugenuma Y, Iwamuro T. Impairment of spermatogenesis in rats by methylmercury : involvement of stage- and cell- specific germ cell apoptosis. Toxicology. 2001;169:25–35.
38. Orisakwe OE, Afonne OJ, Nwobodo E, Asomugha L, Dioka CE. Low-dose mercury induces testicular damage protected by zinc in mice. Eur J Obstet Gynecol Reprod Biol. 2001;95:92–6.
39. Al-Saleh I, Shinwari N, Al-Amodi M. Accumulation of Mercury in Ovaries of Mice After the Application of Skin-lightening Creams. Biol Trace Elem Res. 2009;131:43–54.
40. Alves AC, Monteiro MS, Machado AL, Oliveira M, Bóia A, Correia A, et al. Mercury

levels in parturient and newborns from Aveiro region , Portugal Mercury levels in parturient and newborns from Aveiro region , Portugal. J Toxicol Environ Heal Part A. 2017;80(13–15):697–709.

41. Zheng N, Wang S, Dong W, Hua X, Li Y, Song X, et al. The Toxicological Effects of Mercury Exposure in Marine Fish. Bull Environ Contam Toxicol. 2019;1–7.
42. Zheng N, Wang S, Dong W, Hua X, Li Y, Song X, et al. The Toxicological Effects of Mercury Exposure in Marine Fish. Bull Environ Contam Toxicol. 2019;1–7.
43. Liao CY, Fu JJ, Shi JB, Zhou QF, Yuan CG, Jiang G Bin. Methylmercury accumulation, histopathology effects, and cholinesterase activity alterations in medaka (*Oryzias latipes*) following sublethal exposure to methylmercury chloride. Environ Toxicol Pharmacol. 2006;22(2):225–33.
44. Hill AJ, Teraoka H, Heideman W, Peterson RE. Zebrafish as a model vertebrate for investigating chemical toxicity. Toxicol Sci. 2005;86(1):6–19.
45. Kelkar DS, Provost E, Chaerkady R, Muthusamy B, Manda SS, Subbannayya T, et al. Annotation of the Zebrafish Genome through an Integrated Transcriptomic and Proteomic Analysis. Mol Cell Proteomics. 2014;13(11):3184–98.
46. Yilmaz O, Patinote A, Thao T, Nguyen V, Com E, Lavigne R, et al. Scrambled eggs : Proteomic portraits and novel biomarkers of egg quality in zebrafish (Danio rerio) To cite this version : HAL Id : hal-01640969 Scrambled eggs : Proteomic portraits and novel biomarkers of egg quality in zebrafish (*Danio rerio*). PLoS One. 2017;1–24.
47. Zakaria ZZ, Benslimane FM, Nasrallah GK, Shurbaji S, Younes NN, Mraiche F, et al. Using Zebrafish for Investigating the Molecular Mechanisms of Drug-Induced Cardiotoxicity. Biomed Res Int. 2018;2018:1–10.
48. Wheeler GN, Bra W. Simple Vertebrate Models for Chemical Genetics and Drug Discovery Screens : Lessons From Zebrafish and Xenopus. Dev Dyn. 2009;238:1287–308.
49. Daczewska M, Lewicka A, Dubi M. Zebrafish : A Model for the Study of Toxicants Affecting Muscle Development and Function. Int J Mol Sci. 2016;17:1–22.
50. Zheng JL, Yuan SS, Wu CW, Lv ZM. Acute exposure to waterborne cadmium induced oxidative stress and immunotoxicity in the brain, ovary and liver of zebrafish (Danio rerio). Aquat Toxicol. 2016;180:36–44.
51. Amora M, Giordani S. The utility of zebrafish as a model for screening developmental neurotoxicity. Front Neurosci. 2018;12(976):1–6.
52. Hammerschmidt M. Zebrafish in Endocrine Systems : Recent Advances and Implications for Human Disease. Annu Rev Physiol. 2011;73:183–211.
53. Rupik W, Huszno J, Klag J. Cellular organisation of the mature testes and stages of

spermiogenesis in Danio rerio (Cyprinidae ; Teleostei)— Structural and ultrastructural studies. Micron. 2011;42(8):833–9.

54. Hoo JY, Kumari Y, Shaikh MF, Hue SM, Goh BH. Zebrafish : A Versatile Animal Model for Fertility Research. Biomed Res Int. 2016;1–20.
55. Hardy K. Basic Science in Obstetrics and Gynaecology. 2010. 25-47 p.
56. Mackay S. Gonadal development in mammals at the cellular and molecular levels. Int Rev Cytol. 2000;200:47–99.
57. Sharpe RM, Mckinnell C, Kivlin C, Fisher JS. Proliferation and functional maturation of Sertoli cells , and their relevance to disorders of testis function in adulthood. Reproduction. 2003;125:769–84.
58. Schulz RW, Nóbrega RH, Morais RDVS, Waal PP De, França LR, Bogerd J. Endocrine and paracrine regulation of zebrafish spermatogenesis : the Sertoli cell perspective. Anim Reprod. 2015;12:81–7.
59. Zebrafish A. Thyroid Hormone Stimulates the Proliferation of Sertoli Cells and Single Type A Spermatogonia in. Endocrinology. 2013;154(11):4365–76.
60. Lawrence C. The husbandry of zebrafish (Danio rerio): A review. Aquaculture. 2007;269:1–20.
61. Sessa AK, White R, Houvras Y, Burke C, Pugach E, Baker B, et al. The effect of a depth gradient on the mating behavior, oviposition site preference , and embryo production in the Zebrafish, Danio rerio. Zebrafish. 2008;5(4):335–9.
62. Biology F. Variations of sperm release in three batches of zebrafish. J Fish Biol. 2004;64:475–82.
63. Kimmel CB, Ballard WW, Kimmel SR, Ullmann B, Schilling TF. Stages of Embryonic Development of the Zebrafish. Dev Dyn. 1995;203:253–310.
64. Fuentes R, Fernández J. Ooplasmic Segregation in the Zebrafish Zygote and Early Embryo : Pattern of Ooplasmic Movements and Transport Pathways. Dev Dyn. 2010;239:2172–89.
65. Schier AF, Talbot WS. Molecular Genetics of Axis Formation in Zebrafish. Annu Rev Genet. 2005;39:561–613.
66. Driever W. Axis formation in zebrafish. Curr Opin Genet Dev. 1995;5(5):610–8.
67. Clarkson TW, Magos L. The toxicology of mercury and its chemical compounds. Crit Rev Toxicol. 2006;36(8):609–62.
68. Zhang Q, Li Y, Liu Z, Chen Q. Exposure to mercuric chloride induces developmental damage, oxidative stress and immunotoxicity in zebrafish embryos-larvae. Aquat Toxicol. 2016;181:76–85.
69. Kollár T, Kása E, Ferincz Á, Urbányi B, Csenki-bakos Z, Horváth Á. Development of an in

vitro toxicological test system based on zebrafish (*Danio rerio*) sperm analysis. Environ Sci Pollut Res. 2018;25:14426–36.

70. Zhang QF, Li YW, Liu ZH, Chen QL. Reproductive toxicity of inorganic mercury exposure in adult zebrafish: Histological damage, oxidative stress, and alterations of sex hormone and gene expression in the hypothalamic-pituitary-gonadal axis. Aquat Toxicol. 2016;177:417–24.
71. Zhang Q, Li Y, Liu Z, Chen Q. Exposure to mercuric chloride induces developmental damage , oxidative stress and immunotoxicity in zebrafish embryos-larvae. Aquat Toxicol. 2016;181:76–85.
72. Zhang Q, Li Y, Liu Z, Chen Q. Exposure to mercuric chloride induces developmental damage, oxidative stress and immunotoxicity in zebrafish embryos-larvae. Aquat Toxicol. 2016;181:76–85.
73. Gestel C a. M, Brummelen TC. Incorporation of the biomarker concept in ecotoxicology calls for a redefinition of terms. Ecotoxicology. 1996;5(4):217–25.
74. Oost R Van Der, Porte C. Biomarkers in environmental assessment. 2005. 85-148 p.
75. (NRC) C on BM of the NRC. Biological Markers in Environmental Health. Enviornmental Heal Perspect. 1987;74(1):3–9.
76. World Health Organization. Biomarkers and risk assessment: Concepts and principles. Environ Heal Criteria. 1993;(155):3–82.
77. Grandjean P. Biomarkers in Epidemiology. Clin Chemestry. 1995;41(12):1800–3.
78. Nordberg GF. Biomarkers of exposure , effects and susceptibility in humans and their application in studies of interactions among metals in China. Toxicol Lett. 2010;192:45–9.
79. Livingstone DR. Contaminant-stimulated Reactive Oxygen Species Production and Oxidative Damage in Aquatic Organisms. Mar Pollut Bull. 2001;42(8):656–66.
80. Costantini D, Casagrande S, De Filippis S, Brambilla G, Fanfani A, Tagliavini J, et al. Correlates of oxidative stress in wild kestrel nestlings (*Falco tinnunculus*). J Comp Physiol B Biochem Syst Environ Physiol. 2006;176(4):329–37.
81. Yan SH, Wang JH, Zhu LS, Chen AM, Wang J. Thiamethoxam Induces Oxidative Stress and Antioxidant Response in Zebrafish (*Danio Rerio*) Livers. Environ Toxicol. 2015;2006–15.
82. Oost D, Beyer J, Vermeulen NPE. Fish bioaccumulation and biomarkers in environmental risk assessment : a review. Environ Toxicol Pharmacol. 2003;13:57–149.
83. Wilce MCJ, Parker MW. Structure and function of glutathione S-transferases. Biochim Biophys Acta - Protein Struct Mol Enzymol. 1994 Mar 16 [cited 2019 Jan 7];1205(1):1–18.
84. Bartling D, Radio R, Steiner U, Weiler EW. A glutathione S-transferase with glutathione-

peroxidase activity from Arabidopsis thaliana. Eur J Biochem. 1993;216(2):579–86.

85. Hayes JD, Pulford DJ. The glutathione s-transferase supergene family: Regulation of GST and the contribution of the lsoenzymes to cancer chemoprotection and drug resistance part II. Crit Rev Biochem Mol Biol. 1995;30(6):521–600.
86. Storey KB. Oxidative Stress : Animal Adaptations in Nature. Brazilian J Med Biol Res. 1996;29(12):1715–33.
87. Cappello T, Brandão F, Guilherme S, Santos MA, Maisano M, Mauceri A, et al. Insights into the mechanisms underlying mercury-induced oxidative stress in gills of wild fish (Liza aurata) combining 1 H NMR metabolomics and conventional biochemical assays. Sci Total Environ. 2016;549:13–24.
88. Vieira LR, Gravato C, Soares AMVM, Morgado F, Guilhermino L. Acute effects of copper and mercury on the estuarine fish Pomatoschistus microps : Linking biomarkers to behaviour. Chemosphere. 2009;76(10):1416–27.
89. Monteiro D. RF and, A. K. Inorganic mercury exposure : toxicological effects , oxidative stress biomarkers and bioaccumulation in the tropical freshwater fish matrinxã, Brycon amazonicus (Spix and Agassiz , 1829) matrinxa. Ecotoxicology. 2010;19:105–23.
90. Grotto D, Valentini J, Fillion M, José C, Passos S, Cristina S, et al. Mercury exposure and oxidative stress in communities of the Brazilian Amazon. Sci Total Environ. 2010;408(4):806–11.
91. Macdonald J, Galley HF, Webster NR. Oxidative stress and gene expression in sepsis. Br J Anaesth. 2003;90(2):221–32.
92. Kostelnik A, Pohanka M. Inhibition of acetylcholinesterase and butyrylcholinesterase by a plant secondary metabolite boldine. Biomed Res Int. 2018;2018:1–5.
93. Leomanni A, Schettino T, Calisi A, Lionetto MG. Mercury induced haemocyte alterations in the terrestrial snail Cantareus apertus as novel biomarker. Comp Biochem Physiol Part C. 2016;183–184:20–7.
94. Kais B, Stengel D, Batel A, Braunbeck T. Acetylcholinesterase in zebrafish embryos as a tool to identify neurotoxic effects in sediments. Environ Sci Pollut Res. 2015;22(21):16329–39.
95. Gobi N, Vaseeharan B, Rekha R, Vijayakumar S. Bioaccumulation, cytotoxicity and oxidative stress of the acute exposure selenium in Oreochromis mossambicus. Ecotoxicol Environ Saf. 2018;162:147–59.
96. Maharajan K, Muthulakshmi S, Nataraj B, Ramesh M. Toxicity assessment of pyriproxyfen in vertebrate model zebra fi sh embryos (*Danio rerio*): A multi biomarker study. Aquat Toxicol. 2018;196(October 2017):132–45.

97. Richetti SK, Rosemberg DB, Ventura-lima J, Monserrat JM, Bogo MR, Bonan CD. Acetylcholinesterase activity and antioxidant capacity of zebrafish brain is altered by heavy metal exposure. Neurotoxicology. 2011;32(1):116–22.
98. Behra M., Cousin X., Bertrand C., Vonesch Jean-Luc, Biellmann D. CA& SU. Acetylcholinesterase is required for neuronal and muscular development in the zebrafish embryo. Nat Neurosci. 2002;5:111–8.
99. Forrest ARR, Ravasi T, Taylor D, Huber T, Hume DA, Group RGER, et al. Phosphoregulators : Protein Kinases and Protein Phosphatases of Mouse. Genome Res. 2003;13:1443–54.
100. Korrodi-Gregório L, Esteves SLC, Fardilha M. Protein phosphatase 1 catalytic isoforms: specificity toward interacting proteins. Transl Res. 2014;164(5).
101. Barford D, Das AK, Egloff M. The Structure and Mechanism of Protein Phosphatases: Insights into Catalysis and Regulation. Annu Rev Biophys Mulecular Struct. 1998;27:133–64.
102. Cohen PTW. Novel protein serine/threonine phosphatases: variety is spice of life. Trends Biochem Sci. 1997;22(7):245–51.
103. Wera S, Hemmingst BA. Serine / threonine protein phosphatases. Biochem J. 1995;311:17–29.
104. Kolupaeva V. Serine-threonine protein phosphatases : Lost in translation. BBA - Mol Cell Res. 2019;1866(1):83–9.
105. Fardilha M, Esteves SLC, Cruz OAB, Cruz EF. The Physiological Relevance of Protein Phosphatase 1 and its Interacting Proteins to Health and Disease. Curr Med Chem. 2010;17(33):3996–4017.
106. Shimizu N, Ishitani S, Sato A, Shibuya H, Ishitani T. Hipk2 and PP1c Cooperate to Maintain Dvl Protein Levels Required for Wnt Signal Transduction. CellReports. 2014;8(5):1391–404.
107. Bertolotti A. The split protein phosphatase system. Biochem J. 2018;475:3707–23.
108. Chakrabarti R, Kline D, Lu J, Orth J, Pilder S, Vijayaraghavan S. Analysis of Ppp1cc -Null Mice Suggests a Role for PP1gamma2 in Sperm Morphogenesis. Biol Reprod. 2007;76:992–1001.
109. Takizawa N. Tissue Distribution of Isoforms of Type-1 Protein Phosphatase PP1 in Mouse Tissues and Its Diabetic Alterations. J Biochem. 1994;116(2):411–5.
110. Sinha N, Puri P, Nairn AC, Vijayaraghavan S. Selective Ablation of Ppp1cc Gene in Testicular Germ Cells Causes Oligo- Teratozoospermia and Infertility in Mice. Biol Reprod. 2013;89(5):1–15.

111. Fardilha M, Ferreira M, Pelech S, Vieira S, Rebelo S, Korrodi-Gregorio L, et al. “OMICS” of human sperm: Profiling protein phosphatases. Omi A J Integr Biol. 2013;17(9):460–72.
112. Jayashankar V, Nguyen MJ, Carr BW, Zheng DC, Rosales JB, Rosales B, et al. Protein Phosphatase 1 β Paralogs Encode the Zebrafish Myosin Phosphatase Catalytic Subunit. PLoS One. 2013;8(9):1–19.
113. Dolgova N V., Nehzati S, Macdonald TC, Summers KL, Crawford AM, Krone PH, et al. Disruption of selenium transport and function is a major contributor to mercury toxicity in zebrafish larvae. R Soc Chem. 2019;11(3):621–31.
114. Mendieta-Serrano MA, Schnabel D, Lomelí H, Salas-Vidal E. Spatial and temporal expression of zebrafish glutathione peroxidase 4 a and b genes during early embryo development. Gene Expr Patterns. 2015;19(1–2):98–107.
115. Rong X, Zhou Y, Liu Y, Zhao B, Wang B, Wang C, et al. Glutathione peroxidase 4 inhibits Wnt / β -catenin signaling and regulates dorsal organizer formation in zebrafish embryos. Co Biol. 2017;144:1687–97.
116. OECD. Test No. 236: Fish Embryo Acute Toxicity (FET) Test. OECD; 2013 [cited 2020 Jan 2]. (OECD Guidelines for the Testing of Chemicals, Section 2).
117. Bradford MM. A Rapid and Sensitive Method for the Quantitation Microgram Quantities of Protein Utilizing the Principle of Protein-Dye Binding. Anal Biochem. 1976;72:248–54.
118. Ellman GL, Courtney KD, Andres V, Featherstone R 1007@s001289900286. pd. A new and rapid colorimetric determination of acetylcholinesterase activity. Biochem Pharmacol. 1961;7:88–95.
119. Guilhermino L, Lopes MC, Carvalho AP, Soares AMVM. Acetylcholinesterase Activity in Juveniles of Daphnia magna Straus. Bol Environ Contam Toxicol. 1996;57:979–85.
120. Cribb E, Steven J. Use of a Microplate Reader in an Assay of Glutathione Reductase Using 5,5’-Dithiobis (2-nitrobenzoic Acid). Anal Biochem. 1989;183:195–6.
121. Habig WH, Pabst MJ, Jakoby WB. Glutathione S-Transferases The first enzymatic step in mercapturic ancid formation. J Biol Chem. 1974;249(22):7130–40.
122. Frasco MF, Guilhermino L. Effects of dimethoate and beta-naphthoflavone on selected biomarkers of Poecilia reticulata. Fish Physiol Biochem. 2002;26:149–56.
123. Pundir S, Martin MJ, O’Donovan C. UniProt Tools. Curr Protoc Bioinforma. 2017;53:1–26.
124. Huang W, Cao L, Liu J, Lin L, Dou S. Short-term mercury exposure affecting the development and antioxidant biomarkers of Japanese flounder embryos and larvae. Ecotoxicol Environ Saf. 2010;73(8):1875–83.
125. Ismail A, Yusof S. Effect of mercury and cadmium on early life stages of Java medaka (Oryzias javanicus): A potential tropical test fish. Mar Pollut Bull. 2011;63(5–12):347–9.

126. Perry DM, Weis JS, Weis P. Cytogenetic Effects of Methylmercury in Embryos of the Killifish, Fundulus heteroclitus. Arch Environ Contam Toxicol. 1988;17:569–74.
127. Ismail A, Yusof S. Effect of mercury and cadmium on early life stages of Java medaka (*Oryzias javanicus*): A potential tropical test fish. Mar Pollut Bull. 2011;63(5–12):347–9.
128. Chen Y, Zeng S, Cao Y. Oxidative stress response in zebrafish (*Danio rerio*) gill experimentally exposed to subchronic microcystin-LR. Environ Monit Assess. 2012;184(11):6775–87.
129. Zhang Q, Li Y, Liu Z, Chen Q. Exposure to mercuric chloride induces developmental damage , oxidative stress and immunotoxicity in zebrafish embryos-larvae. Aquat Toxicol. 2016;181:76–85.
130. Dudiki T, Joudeh N, Sinha N, Goswami S, Eisa A, Kline D, et al. The protein phosphatase isoform PP1γ1 substitutes for PP1γ2 to support spermatogenesis but not normal sperm function and fertility. Biol Reprod. 2019;100(3):721–36.
131. Rong X, Zhou Y, Liu Y, Zhao B, Wang B, Wang C, et al. Glutathione peroxidase 4 inhibits Wnt/β-catenin signaling and regulates dorsal organizer formation in zebrafish embryos. Co Biol. 2017;144(9):1687–97.
132. Imai H, Nakagawa Y. Biological significance of phospholipid hydroperoxide glutathione peroxidase (PHGPx, GPx4) in mammalian cells. Free Radic Biol Med. 2003;34(2):145–69.
133. Hermesz E, Ferencz Á. Identification of two phospholipid hydroperoxide glutathione peroxidase (gpx4) genes in common carp. Comp Biochem Physiol Part C. 2009;150(1):101–6.
134. Thisse C, Degrave A, Kryukov G V, Gladyshev VN, Obrecht-pflumio S, Krol A, et al. Spatial and temporal expression patterns of selenoprotein genes during embryogenesis in zebrafish. Gene Expr Patterns. 2003;3:525–32.

Supplementary data

Supplementary Table 1 - Solutions used in the experiments

Western Blot		
Running gel 15% (2 gels, 1.5 mm thickness	ddH_2O	4,280
	Tris-HCl 1,5M pH 8,8	5,000
	Acrylamide 40%	7,360
	Bisacrylamide 2%	2,960
	SDS 10%	0,200
	APS 10%	0,100
	TEMED	0,020
Staking gel 4% (2 gels, 1,5 mm thickness)	ddH_2O	4,736
	Tris-HCl 0,5M pH 6,8	2,000
	Acrylamide 40%	0,784
	Bisacrylamide 2%	0,320
	SDS 10%	0,080
	APS 10%	0,040
	TEMED	0,008
Tris-HCl 1.5 pH 8.8 buffer	For 1 L dissolve 181,5 g of Tris in 800 ml of deionized water. Adjust pH at 8,8 with HCl and make up to 1 L with deionized water.	
Tris-HCl 0.5M pH 6.8 buffer	For 1 L dissolve 60 g of Tris in 800 ml of deionized water. Adjust pH at 6,8 with HCl and make up to 1 L with deionized water.	
10% APS (ammonium persulfate)	For 10 ml of deionized water add 1 g of APS.	
10% SDS (sodium dodecilsulfate)	For 500 ml of deionized water dissolve 50 g of SDS.	
4X LB	For 10 ml add 4 ml of glycerol, 2,5 ml of Tris-HCl 0.5 M pH 6.8, 0,8 g of SDS, 0,2 ml of β-mercaptoethanol and 3,3 ml of deionized water. Add bromophenol blue (a small amount). Keep it at RT for short periods or at 4 ºC for long periods.	
Tris-Gly 10 x stock	For 1 L dissolve 30,30 g of Tris (250 mM) and 144,10 g of Gly (1,92 M) in 1 L of deionized water.	
running buffer	For 1 L add 800 ml of deionized water, 100 ml of Tris-Gly 10x and 10 ml of 10% SDS. Make up to 1 L with deionized water.	
transfer buffer	For 1 L add 100 ml of Tris-Gly 10x to 700 ml of deionized water and 200 ml of methanol.	
10X TBS (Tris buffered saline)	For 1 L dissolve 12,11 g of Tris in deionized water and adjust pH at 8.0. Add 87,665 g of NaCl and make up to 1 L with deionized water.	

1X TBST (TBS + Tween-20)	For 1 L add 100 ml of TBS 10x and 500 µl of Tween-20 to 900 ml of deionized water.
5% BSA in TBST 1x	For 100 mL of solution dissolve 5 g of BSA in TBST 1x.
5% milk in TBST 1x	For 100 mL of solution dissolve 5 g of nonfat milk in TBST 1x.
Ponceau	For 100mL of ponceau staining solution dissolve 0,1 g of pounceau S in 5ml of acid acetic and fill up to 100ml with deionized water.

Supplementary Table 2 – Standards for BCA assay

Tube Name	Volume of BSA (µL)	From Tube	Volume Lysis Buffer (1% SDS) (µL)	Final [BSA] (µg/mL)
A	30.0	BSA stock	0	2000
B	37.5	BSA stock	12.5	1500
C	32.5	BSA stock	32.5	1000
D	17.5	B	17.5	750
E	32.5	C	32.5	500
F	32.5	E	32.5	250
G	32.5	F	32.5	125
H	10.0	G	40.0	25
I	0	-	40.0	0 (Blank)